

pubs.acs.org/JPCA Article

Competition between Solvent···Solvent and Solvent···Solute Interactions in the Microhydration of the Tetrafluoroborate Anion, $BF_4^-(H_2O)_{n=1,2,3,4}$

Published as part of The Journal of Physical Chemistry A virtual special issue "Krishnan Raghavachari Festschrift."

Laura N. Olive, Eric V. Dornshuld, Henry F. Schaefer, III, and Gregory S. Tschumper*



Cite This: J. Phys. Chem. A 2023, 127, 8806-8820



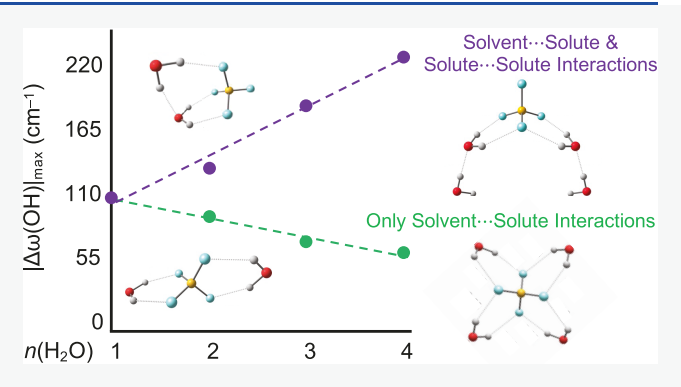
ACCESS

Metrics & More

Article Recommendations

s Supporting Information

ABSTRACT: This study systematically examines the interactions of the tetrafluoroborate anion (BF_4^-) with up to four water molecules $(BF_4^-(H_2O)_{n=1,2,3,4})$. Full geometry optimizations and subsequent harmonic vibrational frequency computations are performed using a variety of density functional theory (DFT) methods (B3LYP, B3LYP-D3BJ, and M06-2X) and the MP2 *ab initio* method with a triple- ζ correlation consistent basis set augmented with diffuse functions on all non-hydrogen atoms (cc-pVTZ for H and aug-cc-pVTZ for B, O, and F; denoted as haTZ). Optimized structures and harmonic vibrational frequencies were also obtained with the CCSD(T) *ab initio* method and the haTZ basis set for the mono- and dihydrate (n=1,2) structures. The 2-body:Many-body (2b:Mb) technique, in which CCSD(T)



computations capture the 1- and 2-body contributions to the interactions and MP2 computations recover all higher-order contributions, was used to extend these demanding computations to the tri- and tetrahydrate (n=3,4) systems. Four, five, and eight new stationary points have been identified for the di-, tri-, and tetrahydrate systems, respectively. The global minimum of the monohydrate adopts a symmetric double ionic hydrogen bond motif with $C_{2\nu}$ symmetry and an electronic dissociation energy of 13.17 kcal mol⁻¹ at the CCSD(T)/haTZ level of theory. This strong solvent···solute interaction, however, competes with solute··· solute interactions in the lowest-energy BF₄⁻(H₂O)_{n=2,3,4} minima that are not seen in the other di-, tri-, or tetrahydrate minima. The latter interactions help increase the 2b:Mb dissociation energies to more than 26, 41, and 51 kcal mol⁻¹ for n=2, 3, and 4, respectively. Structures that form hydrogen bonds between the solvating water molecules also exhibit the largest shifts in the harmonic OH stretching frequencies for the waters of hydration. These shifts can exceed -280 cm⁻¹ relative to an isolated H₂O molecule at the 2b:Mb/haTZ level of theory.

INTRODUCTION

The tetrafluoroborate anion (BF $_4$ ⁻) is popular in stable, room-temperature ionic liquids (RTILs). A variety of practical applications using RTILs were suggested such as use in solar and fuel cells, capacitors, and batteries. The ionic nature of RTILs makes them hygroscopic. The presence of water as an impurity or as a cosolvent can effect the physical properties of RTILs such as viscosity, solubility, electrical conductivity, or even reactivity. Owing to the varying effects of water, the interactions between water and BF $_4$ ⁻-containing RTILs have been the focus of different experimental and theoretical studies. R17-20

 BF_4^- -containing RTILs have been shown to exhibit weak associations with water, but not as weak as those containing the larger SbF_6^- and PF_6^- moieties. Infrared (IR) spectroscopic measurements indicate OH stretching frequen-

cies in the water interacting with the RTIL shift to lower energy (i.e., redshift) with respect to water vapor. The OH antisymmetric stretching mode, ν_3 , and symmetric stretching mode, ν_1 , in water vapor were reported to be 3756 and 3657 cm⁻¹, respectively. The OH shifts in water toward lower energy for these modes ($\Delta\nu_3$ and $\Delta\nu_1$, respectively) were larger with BF₄⁻ ($\Delta\nu_3$ = -116 cm⁻¹ and $\Delta\nu_1$ = -97 cm⁻¹) compared with their SbF₆⁻ ($\Delta\nu_3$ = -93 cm⁻¹ and $\Delta\nu_1$ = -77

Received: June 14, 2023 Revised: August 14, 2023 Published: September 29, 2023





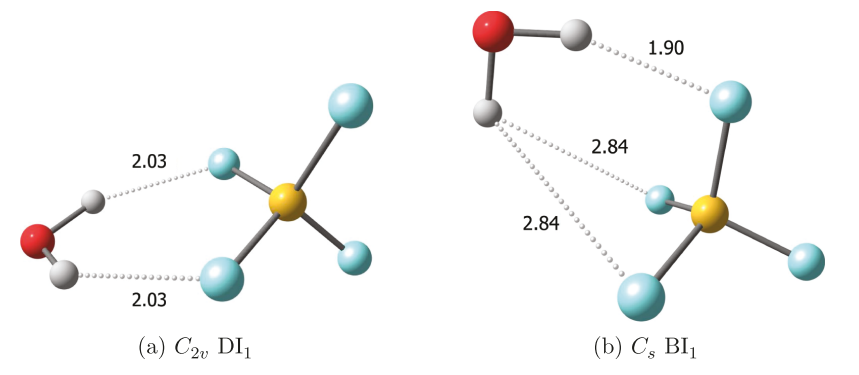


Figure 1. CCSD(T)/haTZ-optimized stationary points of BF₄⁻(H₂O)₁ with select intermolecular R(H···F) distances in Å.

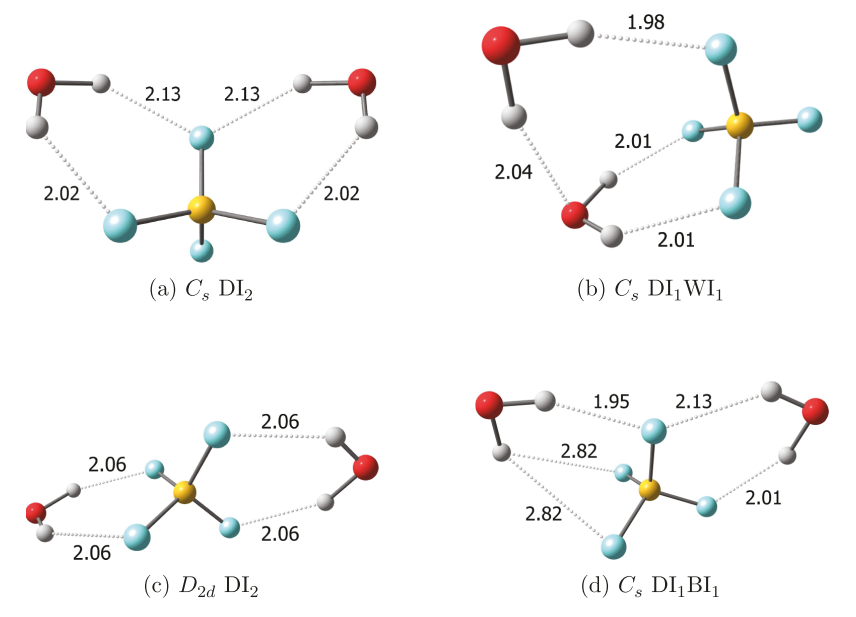


Figure 2. CCSD(T)/haTZ-optimized stationary points of $BF_4^-(H_2O)_2$ with select intermolecular $R(H\cdots F)$ and $R(H\cdots O)$ distances in Å. The 2b:Mb/haTZ-optimized intermolecular $R(H\cdots F)$ and $R(H\cdots F)$ and $R(H\cdots O)$ distances are identical to (or within 0.01 Å) the corresponding CCSD(T) values.

cm⁻¹) and PF₆⁻ ($\Delta\nu_3 = -84~{\rm cm}^{-1}$ and $\Delta\nu_1 = -62~{\rm cm}^{-1}$) counterparts and were unusually large overall. ¹⁷ Corresponding measurements in the same study using singly deuterated water (HDO), a useful probe of ion hydration, confirmed these results. Computational *ab initio* molecular dynamics (AIMD) simulations²³ of aqueous BF₄⁻ and PF₆⁻ probed these unusually large shifts in the absence of a cation. Smiechowski reported OH stretching frequency shifts ($\Delta\nu_{\rm OH}$) to higher energy (i.e., blueshift) of +264 cm⁻¹ for the BF₄⁻ solute and +306 cm⁻¹ for the PF₆⁻ solute when compared with the computed bulk water OH stretching mode of 3320 cm⁻¹.

In ion hydration, when a water molecule binds to small atomic anions, the water generally adopts an asymmetric, single ionic hydrogen bond (SIHB) motif where one hydrogen is attached to the ion and the other hydrogen is free. ^{24–32} For larger systems and molecular anions with extended charge distributions, the symmetric configuration is favored, in which the water molecule binds along the axis of symmetry and adopts a double ionic hydrogen bond (DIHB) motif. ^{29,32–37} The transition from SIHB to DIHB occurs when the hydrogen bond acceptors are separated by about 2.2 Å. ³³ The $C_{2\nu}$ DI₁ structure (Figure 1a) is a monohydrate BF₄⁻ anion where the one (1) water molecule is consistent with the DIHB motif, hence labeled DI₁.

A previous study characterized microsolvated $PF_6^-(H_2O)_{n=1,2}$ conformers with quantum mechanical wave function theory (WFT) and density functional theory (DFT) and examined the OH vibrational shifts of individual H2O molecules allowing for the exploration of not only solute... solvent influences but also solvent···solvent influences on the hydration of this fluorinated anion.³⁸ For the four PF₆ dihydrate minima that only exhibit solvent···solute DIHB contacts, CCSD(T)/haTZ computations indicate the lowestenergy harmonic OH stretches fall in a very narrow window from 3799 to 3801 cm⁻¹ with IR intensities ranging from 54 to 125 km mol⁻¹ (Table S7 from ref 38). The OH stretching frequencies become even smaller when solute···solute interactions are present, such as the water-water hydrogen bond formed in the lowest-energy structure identified for PF₆⁻(H₂O)₂ (C_s WW-Edge-Face in Figure 2 of ref 38.) for which the smallest CCSD(T)/haTZ OH stretching frequency decreases to 3721 cm⁻¹ with a commensurate increase in the corresponding IR intensity to 211 km mol⁻¹. This harmonic OH vibration is only 95 cm⁻¹ larger than that predicted from DFT AIMD simulations of BF₄⁻ hydration. Computed dissociation energies of microhydrated PF₆⁻ were the largest when solvent ··· solvent interactions were present, highlighting the importance of these cooperative effects on the hydration of the anion.

The $BF_4^-(H_2O)_{n=1,2}$ system has been previously characterized with B3LYP and MP2 methods along with basis sets as large as triple- ζ .³⁹ Two following minimum energy structures were reported: a monohydrate complex (denoted as $C_{2\nu}$ DI₁ in Figure 1a) and a dihydrate complex (denoted as D_{2d} DI₂ in Figure 2c). The dihydrate complex was devoid of any solvent… solvent interactions and both waters only interact directly with the solute. The reported MP2 harmonic OH stretching frequency shifts of water (denoted here as $\Delta \omega$ to distinguish from shifts associated with fundamental frequencies, $\Delta \nu$) relative to an isolated water molecule were $\Delta \omega_1 = -41 \text{ cm}^{-1}$ and $\Delta\omega_3 = -110~{\rm cm}^{-1}$ in the monohydrate complex and $\Delta\omega_1$ = -33 cm^{-1} and $\Delta \omega_3 = -95 \text{ cm}^{-1}$ in the dihydrate complex. This study addresses the microsolvated nature of BF₄- but considers complexes with up to four water molecules (i.e., $\mathrm{BF_4}^-(\mathrm{H_2O})_{n=1,2,3,4})$ while employing robust WFT methods and a variety of DFT methods with a flexible, correlation consistent basis set. Computed OH vibrational shifts will be referenced to an isolated water molecule, resulting in a reported redshift, unlike commonly reported blueshifts in works that commonly reference bulk phase water. Solute---solvent and solvent--solvent effects on the hydration of BF₄ will be discussed as well as the dissociation energies of these complexes.

■ COMPUTATIONAL DETAILS

Many of the optimized structures reported here were generated by replicating the hydration patterns previously identified for BF_4^- and related anions such as $BeF_4^{\ 2^-}$, $SO_4^{\ 2^-}$, and $PF_6^{\ -38^-41}$ Additional structures were obtained by systematically introducing additional water molecules along the edges and faces of the BF_4^- tetrahedron to consider unique permutations of solvent---solute and solvent---solvent interactions. All of these starting structures were optimized to one of the various stationary points presented in the Results and Discussion section. Although other minima certainly exist, these should provide a good representation of the lowest-energy hydrogen-bonding motifs for the mono-, di-, tri-, and tetrahydrates of BF_4^- .

For each configuration of the BF $_4$ ⁻(H $_2$ O) $_{n=1,2,3,4}$ clusters and the isolated fragments (BF $_4$ ⁻ and H $_2$ O), fully optimized geometries and corresponding harmonic vibrational frequencies were computed with three different density functional theory (DFT) methods (B3LYP, 42 B3LYP-D3BJ, 42,43 and M06-2X⁴⁴) as well as the MP2⁴⁵ *ab initio* method utilizing the analytic gradients and Hessians available in Gaussian 16.⁴⁶ For the mono- and dihydrate (n=1,2) structures, CCSD(T)-optimized structures were also obtained using the analytic gradients in CFOUR.⁴⁷ The corresponding CCSD(T) harmonic vibrational frequencies were computed from finite differences of gradients. The finite difference procedure was validated with the MP2 method for which the frequencies computed in this manner never differed by more than 0.1 cm⁻¹ from those obtained analytically.

The *N*-body:Many-body (*N*b:Mb) method for noncovalent clusters $^{48-51}$ has been employed to help extend the demanding CCSD(T) computations to the larger complexes in this study (n=2,3,4). In the hierarchy of *N*b:Mb procedures, the multicentered $^{52-56}$ extension of the ONIOM technique $^{57-59}$ is used to recast the traditional many-body expansion of the cluster interaction energy as an ONIOM-based fragmentation scheme. In this procedure, the leading dominant *N* terms in the many-body expansion are computed with an accurate highlevel method, whereas the remaining terms are recovered with

a less demanding but less robust low-level method. For this study, we have selected the 2b:Mb version of the Nb:Mb procedure, which can obtain results nearly identical to those from canonical CCSD(T) computations for these di-, tri-, and tetrahydrate systems. In this implementation, CCSD(T) is used as the high-level (hi) method to describe all 1-body contributions (E_1) and 2-body interactions (ΔE_2) in the cluster while MP2 is used as the low-level (lo) method to recover the remaining (\geq 3-body) interactions via a computation on the entire cluster ($E_{\rm cluster}$). This method gives the following linear expression for the 2b:Mb energy:

$$E_{\text{cluster}}^{\text{2b:Mb}} = E_{\text{cluster}}^{\text{lo}} + E_{1}^{\text{hi}} + \Delta E_{2}^{\text{hi}} - E_{1}^{\text{lo}} - \Delta E_{2}^{\text{lo}}$$
(1)

Analogous expressions can readily be obtained for properties associated with linear operators, such as geometrical derivatives. Consequently, the 2b:Mb geometry optimizations and harmonic vibrational frequency computations 49–51,56 were carried out in this study with Gaussian 16 utilizing its own MP2 analytic gradients and Hessians along with CCSD(T) analytic gradients and numerical Hessians from CFOUR.

A formally equivalent approach was developed by Raghavachari and co-workers. They have used the molecules-in-molecules (MIM) method⁶¹ to efficiently compute MP2 energies 62,63 and DFT spectra for large systems, such as IR,⁶⁴ Raman,⁶⁵ vibrational circular dichroism (VCD),⁶⁶ Raman optical activity (ROA),⁶⁷ and NMR⁶⁸ for large systems. Like other techniques based on the many-body expansion of the interaction energy for noncovalent molecular clusters, 60 these approaches take advantage of the rapid convergence typically observed for this property in such systems. 69-72 Although conceptually simple, the idea of dividing a large system into a number of smaller interacting fragments method is quite powerful. 73-75 As the number of these techniques continues to grow, particularly for noncovalent clusters, two classification schemes have been helpful for identifying their similarities and differences. Richard and Herbert introduced the generalized many-body expansion (GMBE) framework, 76-78 whereas Mayhall and Raghavachari have broadly classified methods into either top-down or bottom-up approaches.⁷⁹ A complete literature review is beyond the scope of this work, but some related efforts include the following: the effective fragment potential (EFP) method, ^{80–82} the fragment molecular orbital (FMO) method, ^{83–85} the molecular tailoring approach (MTA), ^{86,87} the embedded-fragment scheme, ^{88–90} the electrostatically embedded many-body (EE-MB) method, ^{91–93} the generalized energy-based fragmentation (GEBF) method, ^{94–96} the hybrid many-body interaction (HMBI) method, ^{97–99} the extended ONIOM (XO) method, 100,101 the explicit polarization (X-Pol) methods, 102,103 and the stratified approximation many-body approach (SAMBA). 104

All computations for this investigation employed Dunning's correlation consistent triple-ζ basis sets augmented with diffuse functions on all non-hydrogen (or "heavy") atoms (cc-pVTZ for H and aug-cc-pVTZ for B, O, F; denoted as haTZ). ^{105,106} As early as 1993, Del Bene began demonstrating that diffuse functions were not needed on H atoms to reliably characterize the energetics of hydrogen bonding with correlation consistent basis sets, including complexes containing a negatively charged fragment. ^{107,108} In fact, MP2 dissociation energies for the water dimer and trimer tend to be much closer to the complete basis set limit when diffuse functions are omitted from the H atoms. ^{109–111} Those early studies by Del Bene introduced a modified aug' prefix to denote the mixed basis sets where cc-

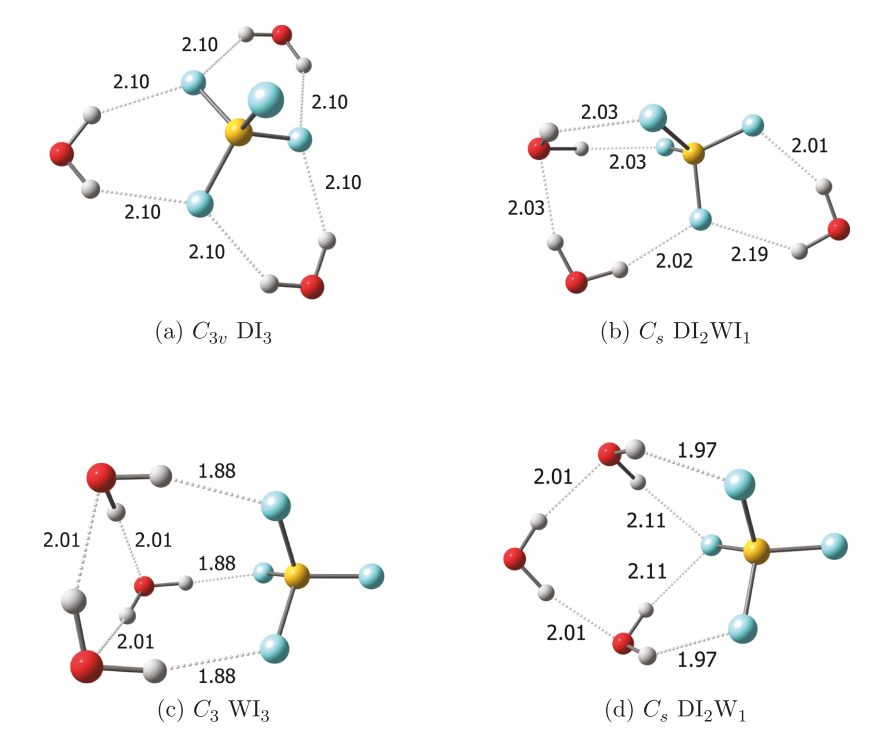


Figure 3. 2b:Mb/haTZ-optimized stationary points of $BF_4^-(H_2O)_3$ with select intermolecular $R(H\cdots F)$ and $R(H\cdots O)$ distances in Å.

pVXZ is used for H and aug-cc-pVXZ is used for the other atomic centers (i.e., aug'cc-pVXZ or simply a'XZ where X is the cardinal number of the basis set). Although still utilized, 40,112 the prime designation in the basis set name has sometimes been adopted in other contexts. Consequently, an alternative heavy-aug-cc-pVXZ or haug-cc-pVXZ (or simply haXZ) notation was introduced around 2007 to indicate that only the basis sets for the "heavy" (i.e., non-hydrogen) atoms were augmented with diffuse functions 56,111,113-115 and that nomenclature has been adopted in a number of important studies on noncovalent interactions from other groups. 116-121 Another naming scheme was introduced in 2011 that uses prefixes based on the months of the calendar year leading up to August (e.g., may-, jun-, jul-, aug-) 122,123 in which jul-cc-pVXZ is equivalent to the earlier aug'-cc-pVXZ and haug-cc-pVXZ designations. Spherical harmonic 5d and 7f basis functions were used rather than their 6d and 10f Cartesian counterparts for all computations, and all DFT computations utilized a dense pruned numerical integration grid composed of 99 radial shells and 590 angular points per shell (corresponding to the UltraFine keyword).

The electronic dissociation energies (D_e) of the complexes were computed via the supermolecular approach given in eq 2.

$$D_{e} = E(BF_{4}^{-}) + nE(H_{2}O) - E([BF_{4}^{-}(H_{2}O)_{n}])$$
 (2)

This scheme for computing the dissociation energies introduces an inconsistency commonly referred to as basis set superposition error (BSSE). To assess the impact of this inconsistency, a counterpoise (CP) procedure was applied to the lowest-energy minima identified for n = 1, defined below in eq 3. 128

$$D_{\rm e}^{\rm CP} = E({\rm dimer}) - \sum_{i=1}^{2} \left[E({\rm fragment}_{i})_{\rm dimer}^{\rm dimer \, basis} + E({\rm fragment}_{i})_{\rm fragment \, basis}^{\rm fragment \, basis} - E({\rm fragment}_{i})_{\rm dimer \, geometry}^{\rm fragment \, basis} \right]$$

$$(3)$$

The extension of this procedure is not uniquely defined for systems with ≥ 3 fragments. However, a detailed protocol described elsewhere ¹¹¹ for flexible fragments was followed for the BF₄⁻(H₂O)_{n=2,3,4} systems.

■ RESULTS AND DISCUSSION

When a water molecule interacts with BF₄-, there are four structural motifs observed for the mono-, di-, tri-, and tetrahydrate stationary points shown in Figures 1-4. The "DI $_{w}$ " label denotes that w water molecules have formed double ionic hydrogen bonds with a pair of fluorine atoms (Figure 1a). This is the same motif that was recently reported for the microsolvation of the isovalent BeF₄²⁻ ion. 40 The "BI_{r"} label denotes that x water molecules have formed one hydrogen bond with one fluorine atom and a separate bifurcated hydrogen bond with two other fluorine atoms (Figure 1b). When two or more water molecules are present, hydrogen bonding between the water molecules can also occur. The "WI_{ν}" label denotes that y water molecules have formed a hydrogen bond with one fluorine atom and a hydrogen bond with another water molecule (Figure 2b). The "W_z" label denotes that z water molecules have formed one or two hydrogen bonds with at least one other water molecule but not the ion (Figure 3d). For each motif, w + x + y + z = n, where n is the number of water molecules present. The Cartesian coordinates and harmonic vibrational frequencies for the mono-, di-, tri-, and tetrahydrated structures are reported in the Supporting Information.

Table 1. Relative Electronic Energies (ΔE in kcal mol⁻¹) and Number of Imaginary Modes (n_i) of the BF₄⁻(H₂O)_{n=1,2,3,4} Structures Optimized with Various Methods and the haTZ Basis Set

structure	n_i	B3LYP	B3LYP-D3BJ	M06-2X	MP2	CCSD(T)	2b:Mb
			n =	1			
$C_{2\nu}$ DI ₁	0	0.00	0.00	0.00	0.00	0.00	
C_s BI ₁	1	1.15	1.27	1.19	1.24	1.28	
			n = 1	2			
D_{2d} DI_2	0	0.00	0.00	0.00	0.00	0.00	0.00
C_s DI ₂	0	0.40	0.36	0.47	0.39	0.39	0.39
$C_s \operatorname{DI_1BI_1}$	1	1.43	1.51	1.45	1.49	1.52	1.52
$C_s DI_1WI_1$	0	-1.03	-1.64	-1.35	-1.32	-1.30	-1.35
			n = 1	3			
$C_{3\nu}$ DI ₃	0	0.00	0.00	0.00	0.00		0.00
$C_s \text{ DI}_2 \text{WI}_1$	0	-2.01	-2.50	-2.43	-2.24		-2.25
$C_s DI_2W_1$	0	-2.90	-3.55	-3.03	-2.95		-2.88
C_3 WI $_3$	0	-5.92	-7.35	-6.61	-6.32		-6.31
			n = -	4			
S_4 DI ₄	0 ^a	0.00	0.00	0.00	0.00		0.00
D_2 DI ₄	1	0.12	0.00	-0.01	0.02		0.00
C_s DI ₄	1 ^b	0.12	0.10	0.19	0.13		0.14
$C_s \text{ DI}_2W_2$	0	-2.47	-1.79	-0.33	-1.13		-0.56
C_s DI ₃ WI ₁	0	-2.13	-2.67	-2.61	-2.42		-2.44
$C_1 \text{ DI}_2 W_2$	0	-3.96	-4.26	-4.49	-3.34		-2.92
$C_s \text{ DI}_2 \text{WI}_2$	0	-3.50	-4.62	-4.43	-4.09		-4.12
$C_1 \text{ DI}_1 \text{WI}_3$	0	-6.78	-8.21	-7.60	-7.20		-7.18
= 1 for M06-2X	$^b n_i = 0$ for B3	SLYP-D3BJ.					

Monohydrate Structures and Relative Energies. In addition to the $C_{2\nu}$ DI₁ minimum reported by Wang, Li, and Han³⁹ (Figure 1a), a second stationary point has been identified in the current work for the monohydrated BF₄⁻ system (Figure 1b). The C_s BI₁ configuration is a transition state lying 1.28 kcal mol⁻¹ above the $C_{2\nu}$ DI₁ structure according to the CCSD(T)/haTZ electronic energy (ΔE values in Table 1). Compared with the monohydrated structures of PF₆⁻, the C_s Face transition state lies 0.30 kcal mol⁻¹ above the $C_{2\nu}$ Edge structure at the CCSD(T)/haTZ level of theory.³⁸

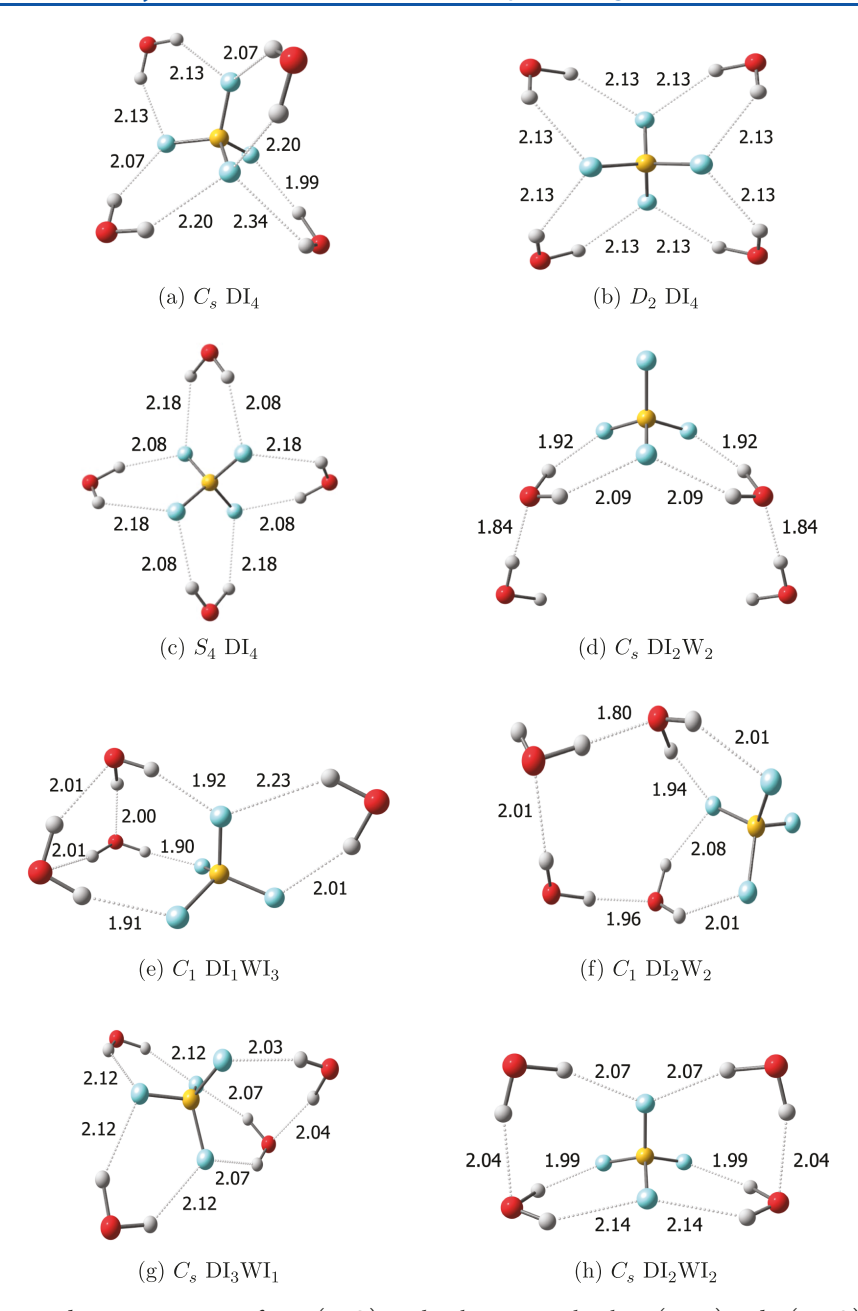
The distance between the F atoms that interact with the H_2O molecule in the $C_{2\nu}$ DI₁ structure (Figure 1a) is 2.0 Å, which is only 0.1 Å smaller than the corresponding distance for the analogous structure of $PF_6^-(H_2O)_1$ (denoted as $C_{2\nu}$ Edge in Figure 1 of ref 38.). Both of these values are similar to but slightly smaller than the usual distance-based threshold of 2.2 Å for the transition between single and double ionic hydrogenbonding motifs.³³ The F···HO angle about the hydrogen bond in the $C_{2\nu}$ DI₁ structure is 143°, similar to analogous angles for other DIHB monohydrates $(146 \pm 2^{\circ})$.³³

Dihydrate Structures and Relative Energies. In addition to the D_{2d} DI₂ minimum characterized in a prior study, ³⁹ three new stationary points were identified with correlated WFT methods (MP2, CCSD(T), and 2b:Mb) for the BF₄⁻(H₂O)₂ system and to our knowledge, these have not been reported before in the literature. These four configurations are shown in Figure 2. For two of the four structures, both waters bridge an edge of the BF₄⁻ tetrahedron that includes the C_s DI₂ and the D_{2d} DI₂ structures (Figure 2a and 2c, respectively). The C_s DI₁BI₁ dihydrate structure (Figure 2d) was generated from the D_{2d} DI₂ configuration by moving one of the water molecules from the edge to an adjacent face. The C_s DI₁WI₁ configuration (Figure 2b) exhibits a completely different hydrogen-bonding topology, with one hydrogen bond

forming between the two water molecules along with three hydrogen bonds between the water molecules and the tetrafluoroborate anion.

The D_{2d} DI₂ structure was used as the reference for the dihydrate relative energies in Table 1 because it has been previously characterized in a prior study as a minimum for $BF_4^-(H_2O)_2^{39}$ The other dihydrate structure with a similar DIHB motif (C_s DI₂) lies 0.39 kcal mol⁻¹ above the D_{2d} DI₂ structure according to the MP2, 2b:Mb, and canonical CCSD(T) relative electronic energies in Table 1. The C_s DI₁BI₁ is a transition state lying 1.49–1.52 kcal mol⁻¹ higher in energy according to the MP2, 2b:Mb, and canonical CCSD(T) results in Table 1. Similar to the hydration of other molecular anions, the introduction of a second water molecule leads to water-water interactions that are significant. 129-133 The newly identified C_s DI₁WI₁ structure that exhibits water…water hydrogen bonding consistently has the lowest MP2, 2b:Mb and canonical CCSD(T) electronic energies and lies 1.30-1.35 kcal mol^{-1} below the D_{2d} DI₂ structure only involving water-ion interactions according to the MP2 and CCSD(T) results in Table 1, respectively. These results could be indicative that the solvent ... solvent interactions between the water molecules could be just as important as the solvent... solute interactions between water and BF₄⁻ in the characterization of the hydration of this ion. The analogous PF₆ structure exhibiting water---water hydrogen bonding (C_s WW-Edge-Face in Figure 2 of ref 38.) lies approximately 2 kcal mol⁻¹ below the other structures only involving water—ion interactions.38

MP2 and CCSD(T) harmonic vibrational frequencies indicate that both of the DI_2 stationary points are minima. The C_s $\mathrm{DI}_1\mathrm{BI}_1$ configuration is a transition state and the C_s $\mathrm{DI}_1\mathrm{WI}_1$ structure appears to be a strong candidate for the global minimum of the $\mathrm{BF}_4^-(\mathrm{H}_2\mathrm{O})_2$ system.



 $\textbf{Figure 4. 2b:} Mb/haTZ-optimized \ stationary \ points \ of \ BF_4^-(H_2O)_4 \ with \ select \ intermolecular \ R(H\cdots F) \ and \ R(H\cdots O) \ distances \ in \ \text{\r{A}}.$

Trihydrate Structures and Relative Energies. Four new stationary points were identified for the $BF_4^-(H_2O)_3$ system with the MP2 and 2b:Mb methods and these configurations are shown in Figure 3. To the best of our knowledge, these structures have not been reported before in the literature, and the MP2 and 2b:Mb harmonic vibrational frequencies indicate each one is a minimum. In the $C_{3\nu}$ DI₃ structure (Figure 3a), all three waters bridge an edge of the BF_4^- tetrahedron. For two of the five structures, all three waters interact with one another. This includes the C_3 WI₃ and C_s DI₂W₁ structures (Figure 3c and 3d, respectively). In the C_s DI₂WI₁ structure (Figure 3b), two water molecules interact with one another, while the third water molecule only forms hydrogen bonds with the ion.

All of the structures that exhibit water···water hydrogen bonding have electronic energies at least 2 kcal mol^{-1} lower than the $C_{3\nu}$ DI₃ structure that has only water—ion interactions.

The C_3 WI₃ and C_s DI₂W₁ structures where multiple hydrogen bonds are formed between the three waters lie lower than the C_s DI₂WI₁ structure that only has one hydrogen bond formed between two of the three waters. The 2b:Mb energetics in Table 1 indicate that the C_s DI₂WI₁ structure lies 2.25 kcal mol⁻¹ lower than the $C_{3\nu}$ DI₃ structure compared with the C_s DI₂W₁ and C_3 WI₃ structures that lie 2.88 and 6.31 kcal mol⁻¹ lower, respectively. These results further demonstrate the importance of solvent····solvent interactions when characterizing the hydration of the BF₄⁻ ion. The C_3 WI₃ structure consistently has the lowest electronic energy and appears to be a strong candidate as the global minimum of the BF₄⁻(H₂O)₃ system.

Tetrahydrate Structures and Relative Energies. Eight new stationary points were identified for the $BF_4^-(H_2O)_4$ system and all eight configurations are shown in Figure 4. To our knowledge, these structures have not been reported before

in the literature. In three of the eight configurations, all four waters bridge an edge of the BF_4^- tetrahedron. This includes the S_4 DI₄ minimum (Figure 4c), and the two other DI₄ structures (C_s and D_2), which are symmetry-unique permutations along the different edges of BF_4^- , and can be seen in Figure 4a and 4b, respectively. All three of the DI₄ structures have very similar electronic energies (within 0.2 kcal mol⁻¹ of each other) at all levels of theory used in this study, but the MP2 and 2b:Mb harmonic vibrational frequencies indicate that the C_s and D_2 stationary points are transition states.

The structures that exhibit water-water hydrogen bonding (Figure 4d-4h) all lie lower than the DI₄ structures that only exhibit water-ion interactions, and they are all minima based on the harmonic vibrational frequencies computed at each level of theory. The C_s DI₂W₂ structure (Figure 4d) and the C_1 DI₂W₂ (Figure 4f) both have two water molecules that form hydrogen bonds with the other two water molecules that bridge an edge of the BF₄⁻ tetrahedron. However, when the symmetry is relaxed from C_s to C_1 in the C_1 DI₂W₂ structure (Figure 4f), a new water water hydrogen bond is formed, which leads to a hydrogen bond bridge being formed between the other two water molecules that have adopted the DIHB motif. The 2b:Mb energetics in Table 1 indicate that the C_1 DI₂W₂ structure lies 2.92 kcal mol⁻¹ lower in energy than the S_4 DI₄ structure, compared with the C_s DI₂W₂ structure that lies 0.56 kcal mol⁻¹ lower. Interestingly, the C_s DI₃WI₁ structure (Figure 4b), which has one water molecule that forms hydrogen bonds to both the ion and to one other water molecule, lies lower in energy than the C_s DI₂W₂ structure that exhibits more water—water interactions. The C_s DI₃WI₁ structure lies 2.44 kcal mol⁻¹ lower than the S_4 DI₄ structure according to the 2b:Mb energetics in Table 1. Two of the four water molecules form hydrogen bonds to both the ion and one other water molecule in the C_s DI₂WI₂ structure (Figure 4c), which lies 4.12 kcal mol⁻¹ below the S₄ DI₄ structure, according to the 2b:Mb results in Table 1. The C_1 DI₁WI₃ structure (Figure 4e) has three out of the four water molecules forming hydrogen bonds to both the ion and each other. It consistently has the lowest electronic energy and is significantly lower than the S_4 DI₄ structure by 7.18 kcal mol⁻¹ according to the 2b:Mb relative energetics. Thus, the C_1 DI₁WI₃ structure appears to be a strong candidate as the global minimum of the BF₄⁻(H₂O)₄ system. As with both the dihydrate and the trihydrate relative energies, we see that the solvent---solvent interactions between the water molecules should also be taken into consideration in addition to the solvent···solute interactions between water and BF₄⁻ in the characterization of the hydration of this ion.

Dissociation Energies. The electronic dissociation energies (D_e) of the optimized minima for the mono-, di-, tri-, and tetrahydrate systems (i.e., the relative energy of the isolated, optimized fragments: one BF_4^- ion and nH_2O molecules) are given in Table 2. According to the MP2 and CCSD(T) results obtained with the haTZ basis set, the monohydrate $C_{2\nu}$ DI₁ structure has a dissociation energy near 13 kcal mol⁻¹ and, as expected, is significantly larger (by more than a factor of 2) than the dissociation energy of the water dimer computed at a comparable level of theory (ca. 5 kcal mol⁻¹). 109,134,135 Furthermore, BF_4^- interacts more strongly with water $(C_{2\nu}$ DI₁; $D_e = 13.17$ kcal mol⁻¹ at the CCSD(T)/haTZ level of theory) than the larger PF_6^- anion ($C_{2\nu}$ Edge; $D_e = 10.55$ kcal mol⁻¹ at the CCSD(T)/haQZ level of theory from ref 38). Interestingly, the additional charge associated

Table 2. Dissociation Energies (in kcal mol⁻¹) Obtained without the CP Procedure for the $BF_4^-(H_2O)_{n=1,2,3,4}$ Minima Optimized with Various Methods and the haTZ Basis Set

		B3LYP-	M06-			
structure	B3LYP	D3BJ	2X	MP2	CCSD(T)	2b:Mb
			n = 1			
$C_{2\nu}$ DI ₁	11.77	12.98	13.84	12.92	13.17	
			n = 2			
D_{2d} DI_2	22.28	24.68	26.34	24.61	25.12	25.11
C_s DI ₂	21.89	24.33	25.87	24.22	24.73	24.73
$C_s \operatorname{DI}_1 \operatorname{WI}_1$	23.31	26.32	27.69	25.93	26.43	26.46
			n = 3			
$C_{3\nu}$ DI ₃	30.61	34.29	36.39	34.16		34.93
$C_s \operatorname{DI_2WI_1}$	32.61	36.79	38.82	36.40		37.18
$C_s \operatorname{DI}_2 W_1$	33.50	37.83	39.42	37.11		37.81
$C_3 WI_3$	36.52	41.64	42.99	40.48		41.24
			n = 4			
S_4 DI ₄	38.41	43.23	45.76	43.07		44.09
$C_s \operatorname{DI_2W_2}$	40.88	45.03	46.09	44.20		44.65
C_s DI ₃ WI ₁	40.54	45.91	48.36	45.49		46.53
$C_1 DI_2W_2$	42.37	47.49	50.25	46.41		47.01
C_s DI ₂ WI ₂	41.91	47.85	50.19	47.16		48.21
$C_1 \text{ DI}_1 \text{WI}_3$	45.18	51.44	53.36	50.27		51.27

with the analogous monohydrate structure of BeF_4^{2-} increases the dissociation energy by a factor of nearly 2.4 according to MP2 computations with the haTZ basis set (12.92 vs 31.00 kcal mol^{-1}).⁴⁰

Perhaps unsurprisingly, the tabulated dissociation energies for the dihydrate structures (Table 2) indicate that the introduction of a second solute···solvent interaction is nearly perfectly additive. For example, when two water molecules attach to different edges of the BF₄⁻ tetrahedron to form the C_s DI_2 and D_{2d} DI_2 minima, the D_e increases by a factor of ≈ 1.9 , or to approximately 25 kcal mol-1, relative to the corresponding value of the monohydrate minimum, $C_{2\nu}$ DI₁, according to the MP2, 2b:Mb and canonical CCSD(T) results in Table 2. Compared with the analogous all-edge structures of $PF_6^-(H_2O)_2$, the D_e increase factor is also ≈ 1.9 relative to the corresponding value of the monohydrate minimum. At the CCSD(T)/haQZ level of theory, the dissociation energies for all-edge dihydrate minima of PF₆⁻ are approximately 20 kcal mol-1. One dihydrate complex was reported for BeF₄²⁻ and has a dissociation energy of 59.37 kcal mol⁻¹ according to MP2/haTZ.⁴⁰ The D_e increase factor is also ≈ 1.9 relative to that of the monohydrate structure.

Moving to the trihydrate structures without solvent···solvent interactions, larger deviations from pairwise additivity are observed when a third water molecule forms a DIHB with the ion. $D_{\rm e}$ for the $C_{3\nu}$ DI $_3$ structure increases by a factor of \approx 2.7 relative to the monohydrate minimum to a value of 34.93 kcal mol $^{-1}$ according to the 2b:Mb/haTZ data in Table 2. For the tetrahydrate DI $_4$ structures, the attenuation is even more pronounced, and $D_{\rm e}$ only increases by a factor of \approx 3.3 relative to the monohydrate minimum, or to 44.09 kcal mol $^{-1}$ as seen in the S_4 DI $_4$ configuration devoid of solvent···solvent contacts. Compared with the one tetrahydrate complex of BeF $_4^{-2}$, the dissociation energy is 105.71 kcal mol $^{-1}$ at the MP2/haTZ level of theory, which gives a similar $D_{\rm e}$ increase factor of \approx 3.4 relative to the monohydrate structure.

The presence of interactions between the solute and solvent molecules can significantly impact the dissociation energies of

Table 3. Harmonic OH Stretching Frequencies (ω in cm⁻¹) for H₂O and BF₄⁻(H₂O)_{n=1,2} Minima Computed with an haTZ Basis Set

structure	Irreps	B3LYP	B3LYP-D3BJ	M06-2X	MP2	CCSD(T)	2b:Mb
$H_2O(\omega)$	a_1	3802	3802	3872	3824	3814	
	b_2	3905	3905	3977	3952	3924	
$C_{2\nu}$ DI_1 (ω)	a_1	3744	3743	3820	3770	3772	
	b_2	3776	3773	3852	3825	3815	
$C_s \operatorname{DI}_2(\omega)$	a"	3740	3746	3828	3774	3778	3778
	a'	3742	3748	3830	3776	3779	3780
	a"	3809	3801	3873	3848	3835	3835
	a'	3813	3806	3879	3853	3839	3839
$C_s \operatorname{DI_1WI_1}(\omega)$	a′	3673	3667	3764	3706	3716	3714
	a′	3721	3719	3793	3746	3750	3750
	a′	3749	3745	3830	3795	3790	3790
	a"	3757	3752	3830	3803	3795	3796
D_{2d} DI ₂ (ω)	b_2	3754	3753	3828	3779	3780	3781
	a_1	3756	3755	3829	3780	3782	3782
	e	3794	3792	3868	3842	3830	3831
	e	3794	3792	3868	3842	3830	3831

Table 4. Harmonic OH Stretching Frequencies (ω in cm⁻¹) for H₂O and BF₄⁻(H₂O)_{n=3} Minima Computed with an haTZ Basis Set

structure	Irreps	B3LYP	B3LYP-D3BJ	M06-2X	MP2	CCSD(T)	2b:Mb
$H_2O(\omega)$	a_1	3802	3802	3872	3824	3814	
	b_2	3905	3905	3977	3952	3924	
$C_{3\nu}$ DI ₃ (ω)	e	3767	3767	3839	3792		3791
	e	3767	3767	3839	3792		3791
	a_1	3770	3770	3843	3795		3794
	a_2	3813	3810	3884	3859		3846
	e	3819	3817	3891	3866		3852
	e	3819	3817	3891	3866		3852
$C_s \operatorname{DI_2WI_1}(\omega)$	a'	3671	3666	3768	3708		3717
	a'	3733	3732	3806	3758		3761
	a'	3740	3750	3834	3778		3783
	a'	3772	3768	3845	3815		3807
	a"	3773	3769	3850	3819		3811
	a'	3828	3819	3886	3865		3850
$C_3 \text{ WI}_3 (\omega)$	a	3589	3575	3691	3618		3635
	e	3640	3631	3736	3671		3683
	e	3640	3631	3736	3671		3683
	e	3688	3681	3785	3737		3738
	e	3688	3681	3785	3737		3738
	a	3707	3702	3801	3753		3754
$C_s \operatorname{DI}_2 W_1(\omega)$	a'	3636	3634	3740	3672		3685
	a"	3646	3677	3779	3731		3739
	a′	3697	3723	3816	3755		3766
	a"	3743	3724	3819	3768		3774
	a"	3779	3794	3855	3835		3821
	a'	3839	3800	3865	3841		3828

the complex. An almost perfectly pairwise additive increase close to exactly 2 is observed for the dissociation energy of the C_s DI₁WI₁ structure relative to the monohydrate minimum, $C_{2\nu}$ DI₁. In comparison to the C_s WW-Edge-Face structure of PF₆⁻(H₂O)₂, cooperative effects were displayed with the water---water hydrogen bonding that enhanced the D_e to greater than 22 kcal mol⁻¹, or by a factor of \approx 2.1. 38

In the trihydrate complexes, the C_3 WI₃ configuration that contains both solute···solute and solvent···solvent interactions has the lowest D_e for all levels of theory. When the three waters are able to interact with two neighboring water molecules as well as have a direct interaction with the solute anion, the

2b:Mb dissociation energy is $41.24 \text{ kcal mol}^{-1}$. Large dissociation energies are also observed for the other trihydrate structures that contain both solute···solvent and solvent··· solvent interactions. The D_e increases by a factor of ≈ 3.1 , which is larger than the increase of ≈ 2.7 , as seen in the DIHB motif.

A similar trend is seen with the tetrahydrate structures. The configurations with numerous solute····solvent and solvent···· solvent interactions lead to larger $D_{\rm e}$. In fact, the C_1 DI₁WI₃ complex, consisting of four water molecules interacting with the anion and three water molecules directly interacting with two neighboring molecules, gives the largest 2b:Mb $D_{\rm e}$ of

51.27 kcal mol⁻¹, 7.18 kcal mol⁻¹ stronger than when solvent··· solvent interactions are not present. Compared with the DIHB motif with an increase factor of \approx 3.3, the $D_{\rm e}$ increases by a factor of \approx 3.9.

When the appropriate CP procedure is applied to the lowest-energy structures identified for the mono-, di-, tri-, and tetrahydrate systems ($C_{2\nu}$ DI₁, C_s DI₁WI₁, C_3 WI₃, and C_1 DI₁WI₃, respectively), the MP2/haTZ dissociation energies decrease by less than 5–6% for all four configurations. All dissociation energies computed with the CP procedure can be found in the Supporting Information.

Vibrational Frequencies. The first two rows of Tables 3 and 4 contain the harmonic symmetric (a_1) and antisymmetric (b_2) OH stretching frequencies (ω) computed for an isolated water molecule. As a water molecule binds to an edge of the BF₄⁻ tetrahedron, the OH···F hydrogen bonds perturb the OH stretching vibrations of the water molecule, which induces a shift in the corresponding frequency $(\Delta\omega)$. For example, in the $C_{2\nu}$ DI₁ monohydrate structure, the energy of the symmetric a_1 stretching mode decreases by 41 cm⁻¹ and that of the antisymmetric b_2 mode decreases by 110 cm⁻¹ according to the CCSD(T)/haTZ results reported in Table 3.

In the DI₂ dihydrate minima (C_s and D_{2d}), where two water molecules bind to different edges of the anion tetrahedron, the magnitudes of the vibrational frequency shifts are smaller than those reported for the monohydrate. According to the CCSD(T)/haTZ harmonic vibrational frequencies in Table 3, the OH stretching frequencies shift to lower energy by -34 ± 2 and -90 ± 5 cm⁻¹ for the symmetric and antisymmetric modes, respectively, in the two DI₂ dihydrate minima (C_s and D_{2d}). The shifts are slightly larger than the corresponding changes seen in PF₆⁻(H₂O)₂, where the symmetric OH stretch shifted to lower energy by -19 ± 7 cm⁻¹, and the antisymmetric OH stretch shifted to lower energy by -75 ± 14 cm⁻¹, ³⁸

The C_s DI₁WI₁ structure has a different hydrogen bond topology than that of the DI₂ structures and, therefore, exhibits much larger OH stretching frequency shifts than that of the DI₂ minima. According to the CCSD(T)/haTZ harmonic vibrational frequencies in Table 3, all but one of the OH stretching modes shifts by at least 95 cm⁻¹. The $\Delta\omega$ value of -64 cm^{-1} is associated with the mode that is dominated by the synchronous OH stretching motion in the water molecule that accepts the hydrogen bond from the other water molecule. In contrast, the $\Delta\omega$ value of $-98~{\rm cm}^{-1}$ can be seen for the water molecule that donates the hydrogen bond. For the asynchronous stretching modes associated with the donor and acceptor of the hydrogen bond, the Δ values are -134 and -129 cm⁻¹, respectively. A similar trend is seen for the analogous C_s WW-Edge-Face dihydrate structure of PF_6^{-38} although three of the four shifts are smaller in magnitude by approximately 30 cm⁻¹ according to the CCSD(T)/haTZ harmonic frequencies reported in Table S7 from ref 38.

The magnitudes of the vibrational frequency shifts in systems where three water molecules bind to different edges of the anion tetrahedron, as seen in the DI₃ trihydrate minimum ($C_{3\nu}$), are smaller than those reported for the monoand dihydrate. According to the 2b:Mb/haTZ harmonic vibrational frequencies in Table 4, the symmetric OH stretch shifts to a lower energy by -21 ± 2 cm⁻¹, and the antisymmetric OH stretch shifts to a lower energy by -75 ± 3 cm⁻¹. As seen with the C_s DI₁WI₁ dihydrate that exhibits water···water hydrogen bonding, all of the remaining trihydrate

structures also exhibit water···water hydrogen bonding, which induces much larger OH stretching frequency shifts than that of the DI_3 minimum. According to the 2b:Mb/haTZ level of theory, the C_3 WI $_3$ structure where all three waters interact with each other exhibits the largest OH stretching frequency shifts. The largest shifts of the OH stretches are approximately $-180~\mathrm{cm}^{-1}$ for vibrations regardless of whether they have symmetric or antisymmetric character.

As four water molecules bind to different edges of the anion tetrahedron in the DI_4 tetrahydrate minimum (S_4) , the magnitudes of the $\Delta\omega$ values are the smallest for the entire $DI_{n=1-4}$ series of minima that exhibit only DIHB interactions. According to the 2b:Mb/haTZ harmonic vibrational frequencies in Table 5, the symmetric OH stretches shift to lower energy by -16 ± 2 cm⁻¹, and the antisymmetric OH stretches shift to lower energy by -61 ± 4 cm⁻¹. As shown before, the structures with water-water hydrogen bonding induce much larger OH stretching frequency shifts. At the 2b:Mb/haTZ level of theory, the C₁ DI₂W₂ structure that forms a bridge between all four molecules exhibits the largest OH stretching frequency shifts with a symmetric character of -281 cm⁻¹. However, the C_1 DI₁WI₃ structure that has three out of the four water molecules interacting with each other exhibits the largest OH stretching frequency shifts with an antisymmetric character of -167 cm⁻¹.

Due to solvent---solute interactions, vibrational frequency shifts are also induced in the BF stretching modes of the tetrafluoroborate anion. However, these shifts tend to be slightly smaller. In the $C_{2\nu}$ DI₁ monohydrate structure, the CCSD(T)/haTZ harmonic vibrational frequencies demonstrate that one of the BF stretching frequencies shifts by -50 cm⁻¹ to lower energy while another shifts by +30 cm⁻¹ to higher energy. The other two stretching modes shift by -6cm⁻¹. These shifts are much larger than those observed for the PF stretching modes.³⁸ When a second water molecule is added, the frequency shifts in the C_s DI₂ and C_s DI₁BI₁ structures are similar to the monohydrate shifts. However, the CCSD(T)/haTZ frequency shifts do not exceed ± 11 cm⁻¹ for the D_{2d} DI_2 structure. When a third or fourth water molecule is added, the frequency shifts are similar to those of the mono- and dihydrate structures. The computed harmonic vibrational frequencies and corresponding IR intensities can be found in the Supporting Information.

Performance of B3LYP, B3LYP-D3BJ, M06-2X, and MP2. The average absolute deviations (AvgAD) and max absolute deviations (MaxAD) of the relative and dissociation energies (in kcal mol⁻¹), as well as the harmonic vibrational frequencies of the OH stretching modes (in cm⁻¹) computed with B3LYP, B3LYP-D3BJ, M06-2X, and MP2 from CCSD(T) for n = 1, 2 and 2b:Mb for n = 3, 4 are given in Table 6. The column N denotes the number of values used for determining the AvgAD and MaxAD. For the relative energies, N is the number of structures identified, excluding the reference structure. As for the dissociation energies, N is the number of minimum energy structures. For the harmonic vibrational frequencies of the OH stretching modes, N is the number of OH stretching modes associated with all of the minimum energy structures.

When comparing the performances of the DFT methods and MP2, there is one clear top performer for dissociation energies. B3LYP-D3BJ consistently gives the smallest AvgAD and MaxAD values for n > 1, even outperforming MP2. B3LYP performed the worst and always gave the largest AvgAD and

Table 5. Harmonic OH Stretching Frequencies (ω in cm⁻¹) for BF₄⁻(H₂O)_{n=4} Minima Computed with an haTZ Basis Set

		Day 110	B3LYP-	M06-	1 500	21.10
structure	Irreps	B3LYP	D3BJ	2X	MP2	2b:Mb
$C_s \operatorname{DI_3WI_1}(\omega)$	a′	3680	3675	3774	3716	3725
	a′	3748	3747	3817	3771	3772
	a"	3773	3773	3845	3797	3796
	a′	3775	3775	3848	3799	3798
	a′	3781	3777	3857	3824	3816
	a"	3796	3794	3866	3841	3831
	a"	3825	3823	3898	3871	3857
	a′	3828	3827	3902	3875	3861
$C_s \operatorname{DI_2WI_2}(\omega)$	a"	3671	3669	3772	3711	3721
	a′	3673	3671	3774	3713	3723
	a"	3719	3730	3812	3757	3764
	a′	3721	3732	3814	3759	3765
	a"	3786	3781	3857	3826	3817
	a′	3794	3790	3863	3835	3826
	a"	3804	3795	3867	3840	3828
	a′	3807	3799	3869	3844	3831
$C_s \operatorname{DI}_2 W_2(\omega)$	a"	3505	3492	3614	3555	3588
	a'	3509	3496	3618	3559	3592
	a"	3694	3703	3801	3735	3750
	a′	3698	3707	3804	3739	3753
	a"	3797	3786	3852	3828	3818
	a'	3802	3791	3860	3834	3824
	a"	3868	3868	3938	3908	3882
	a′	3868	3868	3939	3909	3883
$C_1 \operatorname{DI}_1 \operatorname{WI}_3 (\omega)$	a	3585	3569	3685	3616	3634
	a	3638	3628	3736	3674	3686
	a	3641	3631	3738	3676	3688
	a	3710	3704	3798	3754	3754
	a	3713	3708	3802	3757	3757
	a	3730	3728	3819	3774	3774
	a	3736	3750	3837	3779	3785
()	a	3840	3830	3896	3875	3858
S_4 DI ₄ (ω)	e	3728	3769	3847	3789	3796
	e	3728	3770	3849	3790	3797
	Ь	3729	3770	3849	3790	3797
	a	3732	3772	3853	3793	3800
	a	3851	3829	3898	3877	3859
	e	3851	3832	3904	3881	3863
	e	3851	3832	3904	3881	3863
a press ()	Ь	3853	3836	3909	3885	3867
$C_1 \operatorname{DI}_2 W_2 (\omega)$	a	3437	3422	3506	3491	3533
	a	3629	3620	3716	3660	3676
	a	3692	3692	3753	3738	3752
	a	3702	3719	3757	3752	3759
	a	3736	3746	3784	3773	3780
	a	3773	3748	3813	3804	3798
	a	3809	3797	3837	3845	3833
	a	3865	3865	3927	3902	3877

MaxAD results of all of the methods, with the latter ranging from 1.40 kcal mol^{-1} for n = 1 to 6.30 kcal mol^{-1} for n = 4. Those trends do not, however, extend to the relative energies where MP2 clearly has the advantage and M06-2X tends to yield the smallest AvgADs for the DFT methods but not necessarily the smallest MaxADs. Similarly, the three DFT methods did not perform as well as MP2 when characterizing the harmonic vibrational frequencies of the OH stretching modes. On average, all of the DFT methods predict larger

shifts by about 40 cm⁻¹. Although the MaxADs for B3LYP and B3LYP-D3BJ grew with the size of the cluster (up to 96 and 111 cm⁻¹, respectively), the MaxAD for M06-2X remained remarkably consistent from n = 1 to n = 4.

An additional dihydrate structure (C_s DI₁W₁; whose Cartesian coordinates are in the Supporting Information) was located only at the B3LYP/haTZ level of theory. This structure is characterized by a single water molecule only interacting with the other water molecule and does not form any hydrogen bonds with the ion. All other levels of theory were optimized to the C_s DI₁WI₁ structure. Additionally, for the trihydrate structures, only the B3LYP and M06-2X methods located the C_1 DI₂W₁ structure (whose Cartesian coordinates are in the Supporting Information). Similar to the C_s DI₁W₁ dihydrate structure, one of the water molecules is only interacting with the other water molecule, and no hydrogen bonds are formed with the ion. The B3LYP-D3BJ and MP2 methods did not locate the C_1 DI₂W₁ structure and instead converged to the C_s DI₂W₁ structure.

CONCLUSIONS

Low-energy configurations of the $BF_4^-(H_2O)_{n=1,2,3,4}$ systems have been identified with the MP2, canonical CCSD(T), and 2b:Mb ab initio WFT methods in conjunction with the haTZ basis set. Two low-lying stationary points have been found for the $BF_4^-(H_2O)_1$ system, which includes the C_{2v} DI_1 minimum and the C_s BI₁ transition state. For the BF₄⁻(H₂O)₂ system, three minima and one transition state have been identified, with the lowest-energy minimum being 1.30 kcal mol⁻¹ lower than the D_{2d} DI₂ structure at the CCSD(T)/haTZ level of theory. Four new minima have been identified for the $BF_4^-(H_2O)_3$ system, with the lowest-energy minimum being 6.31 kcal mol⁻¹ lower than the $C_{3\nu}$ DI₃ structure at the 2b:Mb/ haTZ level of theory. For the BF₄-(H₂O)₄ system, six new minima and two new transition states have been identified, with the lowest-energy minimum being 7.18 kcal mol⁻¹ lower than the S₄ DI₄ structure at the 2b:Mb/haTZ level of theory.

The CCSD(T)/haTZ electronic dissociation energy is larger than 13 kcal mol $^{-1}$ for the $C_{2\nu}$ DI $_1$ monohydrate minimum. When the number of water molecules to form the dihydrate structures is increased, this interaction is almost perfectly additive in the D_{2d} DI $_2$ and C_s DI $_2$ minima. For the trihydrate $C_{3\nu}$ DI $_3$ minimum and the tetrahydrate S_4 DI $_4$ minimum, the D_e increases by a factor of \approx 2.7 and \approx 3.3 relative to the monohydrate, respectively. However, when the water molecules interact with one another and form hydrogen bonds, cooperative effects manifest and are observed, and the D_e increases to larger than 26, 41, and 51 kcal mol $^{-1}$ in the di-, tri, and tetrahydrate structures, respectively. For comparison, the D_e is about 5 kcal mol $^{-1}$ for the water dimer 109,135 and approaches 16 kcal mol $^{-1}$ for the water trimer.

Relative to the a_1 and b_2 modes for an isolated H_2O molecule, the solvent···solute interactions induce significant shifts in the harmonic OH stretching frequencies of the hydrating water molecule(s). In the monohydrate minimum $(C_{2\nu} \, \mathrm{DI}_1)$, the $\mathrm{CCSD}(\mathrm{T})/\mathrm{haTZ}$ symmetric and antisymmetric OH stretching frequencies shift by -41 and -110 cm⁻¹, respectively. Similar modest $\Delta\omega$ values are also observed in the $D_{2d} \, \mathrm{DI}_2$, $C_{3\nu} \, \mathrm{DI}_3$, and $S_4 \, \mathrm{DI}_4$ minima of $\mathrm{BF_4}^-(\mathrm{H_2O})_{n=2,3,4}$. The most significant vibrational shifts are seen when the solvent molecules interact with one another and the ion. In the $C_s \, \mathrm{DI}_1 \mathrm{WI}_1$ structure, the $\mathrm{CCSD}(\mathrm{T})/\mathrm{haTZ}$ synchronous and asynchronous OH stretching modes shift by as much as -98

Table 6. Average Absolute Deviations (AvgAD) and Max Absolute Deviations (MaxAD) of the Relative Energies (in kcal mol⁻¹), Dissociation Energies (in kcal mol⁻¹), and the Harmonic OH Stretching Frequencies (in cm⁻¹) Computed with DFT and MP2 from CCSD(T) for n = 1, 2 and 2b:Mb for n = 3, 4^a

	relative energies				dissociation ene	rgies	OH stretching frequencies		
	N	AvgAD	MaxAD	N	AvgAD	MaxAD	N	AvgAD	MaxAI
				n =	1				
B3LYP	1		0.12	1		1.40	2	33	38
B3LYP-D3BJ	1		0.01	1		0.19	2	36	42
M06-2X	1		0.09	1		0.67	2	42	47
MP2	1		0.04	1		0.25	2	6	10
				n =	2				
B3LYP	3	0.12	0.27	3	2.93	3.12	12	34	43
B3LYP-D3BJ	3	0.13	0.33	3	0.32	0.44	12	36	49
M06-2X	3	0.06	0.08	3	1.21	1.26	12	43	51
MP2	3	0.02	0.03	3	0.51	0.52	12	7	14
				n =	3				
B3LYP	3	0.22	0.39	4	4.48	4.71	24	40	93
B3LYP-D3BJ	3	0.65	1.04	4	0.36	0.64	24	41	62
M06-2X	3	0.21	0.30	4	1.62	1.76	24	45	56
MP2	3	0.03	0.07	4	0.75	0.78	24	8	17
				n =	4				
B3LYP	7	0.63	1.92	6	5.41	6.30	48	40	96
B3LYP-D3BJ	7	0.63	1.34	7	0.53	0.85	56	39	111
M06-2X	7	0.40	1.57	5	2.12	3.24	40	39	56
MP2	7	0.15	0.57	6	0.86	1.05	48	12	42

^aThe column N denotes the number of values used for determining the AvgAD and MaxAD.

and -134 cm^{-1} , respectively. Even larger shifts are seen in the trihydrate and tetrahydrate systems. In the C_3 WI₃ structure, the CCSD(T)/haTZ synchronous and asynchronous OH stretching modes shift by as much as -179 and -186 cm⁻¹, respectively.

The lowest-energy harmonic OH stretching frequency for the C₃ WI₃ minimum of BF₄⁻(H₂O)₃ is computed to be 3635 and 3589 cm⁻¹ at the 2b:Mb/haTZ and B3LYP/haTZ levels of theory, respectively. The B3LYP/haTZ harmonic value is only 5 cm⁻¹ larger than the results from DFT AIMD simulations that predicted a shift of +264 cm⁻¹ relative to bulk water.²³ The C₁ DI₁WI₃ tetrahydrate structure also has frequencies that approach the DFT AIMD result with the lowest-energy harmonic OH stretching frequency computed as 3634 and 3638 cm⁻¹ at the 2b:Mb/haTZ and B3LYP/haTZ levels of theory. This work indicates the importance of solvent···solvent interactions when describing the hydration of BF₄⁻ and demonstrates that solvent···solute interactions alone do not encapsulate the total hydration of BF₄⁻. In order to identify the lowest-energy structures and to completely capture the observed spectroscopic shifts, these solvent···solvent interactions must be considered, as reported here.

ASSOCIATED CONTENT

Supporting Information

The Supporting Information is available free of charge at https://pubs.acs.org/doi/10.1021/acs.jpca.3c04014.

Cartesian coordinates, electronic dissociation energies computed with the CP procedure, harmonic vibrational frequencies, and IR intensities (PDF)

AUTHOR INFORMATION

Corresponding Author

Gregory S. Tschumper — Department of Chemistry and Biochemistry, University of Mississippi, University, Mississippi 38677, United States; orcid.org/0000-0002-3933-2200; Phone: +1 (662) 915-7301; Email: tschumpr@olemiss.edu

Authors

Laura N. Olive – Center for Computational Quantum Chemistry, University of Georgia, Athens, Georgia 30602, United States

Eric V. Dornshuld — Department of Chemistry, Mississippi State University, Mississippi State, Mississippi 39762, United States; © orcid.org/0000-0002-1112-9526

Henry F. Schaefer, III — Center for Computational Quantum Chemistry, University of Georgia, Athens, Georgia 30602, United States; orcid.org/0000-0003-0252-2083

Complete contact information is available at: https://pubs.acs.org/10.1021/acs.jpca.3c04014

Notes

The authors declare no competing financial interest.

ACKNOWLEDGMENTS

The authors acknowledge the Mississippi Center for Supercomputing Research for access to their computational resources. This work was funded in part by the National Science Foundation (CHE-1757888, CHE-2154403). L.N.O. acknowledges the NSF for a Graduate Research Fellowship (NSF Award 1842396). The research at Georgia was supported by the U.S. Department of Energy, Basic Energy Sciences, Division of Chemistry, and the Computational and Theoretical Chemistry (CTC) program.

REFERENCES

- (1) Wang, Y.-L.; Li, B.; Sarman, S.; Mocci, F.; Lu, Z.-Y.; Yuan, J.; Laaksonen, A.; Fayer, M. D. Microstructural and Dynamical Heterogeneities in Ionic Liquids. *Chem. Rev.* **2020**, *120*, 5798–5877.
- (2) Papageorgiou, N.; Athanassov, Y.; Armand, M.; Bonhote, P.; Pettersson, H.; Azam, A.; Grätzel, M. The Performance and Stability of Ambient Temperature Molten Salts for Solar Cell Applications. *J. Electrochem. Soc.* **1996**, *143*, 3099–3108.
- (3) Matsumoto, H.; Matsuda, T.; Tsuda, T.; Hagiwara, R.; Ito, Y.; Miyazaki, Y. The Application of Room Temperature Molten Salt with Low Viscosity to the Electrolyte for Dye-Sensitized Solar Cell. *Chem. Lett.* **2001**, *30*, 26–27.
- (4) Doyle, M.; Choi, S. K.; Proulx, G. High-Temperature Proton Conducting Membranes Based on Perfluorinated Ionomer Membrane-Ionic Liquid Composites. *J. Electrochem. Soc.* **2000**, 147, 34.
- (5) Nanjundiah, C.; McDevitt, S. F.; Koch, V. R. Differential Capacitance Measurements in Solvent-Free Ionic Liquids at Hg and C Interfaces. *J. Electrochem. Soc.* **1997**, *144*, 3392–3397.
- (6) Carlin, R. T.; Long, H. C. D.; Fuller, J.; Trulove, P. C. Dual Intercalating Molten Electrolyte Batteries. *J. Electrochem. Soc.* **1994**, 141, L73–L76.
- (7) Maiti, A.; Kumar, A.; Rogers, R. D. Water-clustering in hygroscopic ionic liquids—an implicit solvent analysis. *Phys. Chem. Chem. Phys.* **2012**, *14*, 5139–5146.
- (8) Huddleston, J. G.; Visser, A. E.; Reichert, W. M.; Willauer, H. D.; Broker, G. A.; Rogers, R. D. Characterization and comparison of hydrophilic and hydrophobic room temperature ionic liquids incorporating the imidazolium cation. *Green Chem.* **2001**, *3*, 156–164.
- (9) Wang, J.; Tian, Y.; Zhao, Y.; Zhuo, K. A volumetric and viscosity study for the mixtures of 1-n-butyl-3-methylimidazolium tetrafluor-oborate ionic liquid with acetonitrile, dichloromethane, 2-butanone and N, N dimethylformamide. *Green Chem.* **2003**, *5*, 618–622.
- (10) Widegren, J. A.; Saurer, E. M.; Marsh, K. N.; Magee, J. W. Electrolytic conductivity of four imidazolium-based room-temperature ionic liquids and the effect of a water impurity. *J. Chem. Thermodyn.* **2005**, *37*, 569–575.
- (11) Brown, R. A.; Pollet, P.; McKoon, E.; Eckert, C. A.; Liotta, C. L.; Jessop, P. G. Asymmetric Hydrogenation and Catalyst Recycling Using Ionic Liquid and Supercritical Carbon Dioxide. *J. Am. Chem. Soc.* 2001, 123, 1254–1255.
- (12) Najdanovic-Visak, V.; Esperanca, J. M. S. S.; Rebelo, L. P. N.; Nunes da Ponte, M.; Guedes, H. J. R.; Seddon, K. R.; de Sousa, H. C.; Szydlowski, J. Pressure, Isotope, and Water Co-solvent Effects in Liquid-Liquid Equilibria of (Ionic Liquid + Alcohol) Systems. *J. Phys. Chem. B* **2003**, *107*, 12797–12807.
- (13) Widegren, J. A.; Laesecke, A.; Magee, J. W. The effect of dissolved water on the viscosities of hydrophobic room-temperature ionic liquids. *Chem. Commun.* **2005**, 1610–1612.
- (14) Gómez, E.; González, B.; Domínguez, A.; Tojo, E.; Tojo, J. Dynamic Viscosities of a Series of 1-Alkyl-3-methylimidazolium Chloride Ionic Liquids and Their Binary Mixtures with Water at Several Temperatures. *J. Chem. Eng. Data* **2006**, *51*, 696–701.
- (15) Yang, J.-Z.; Tong, J.; Li, J.-B.; Li, J.-G.; Tong, J. Surface tension of pure and water-containing ionic liquid C₅MIBF₄ (1-methyl-3-pentylimidazolium tetrafluoroborate). *J. Collid Interface Sci.* **2007**, 313, 374–377.
- (16) Kanakubo, M.; Umecky, T.; Aizawa, T.; Kurata, Y. Water-induced Acceleration of Transport Properties in Hydrophobic 1-Butyl-3-methylimidazolium Hexafluorophosphate Ionic Liquid. *Chem. Lett.* **2005**, *34*, *324*–*325*.
- (17) Cammarata, L.; Kazarian, S. G.; Salter, P. A.; Welton, T. Molecular states of water in room temperature ionic liquids. *Phys. Chem. Chem. Phys.* **2001**, *3*, 5192–5200.
- (18) Danten, Y.; Cabaço, M. I.; Besnard, M. Interaction of Water Highly Diluted in 1-Alkyl-3-methyl Imidazolium Ionic Liquids with the PF₆⁻ and BF₄⁻ Anions. *J. Phys. Chem. A* **2009**, *113*, 2873–2889.
- (19) Schenk, J.; Panne, U.; Albrecht, M. Interaction of Levitated Ionic Liquid Droplets with Water. *J. Phys. Chem. B* **2012**, *116*, 14171–14177.

- (20) Grabowski, S. J. Hydrogen Bonds with BF₄⁻ Anion as a Proton Acceptor. *Crystals* **2020**, *10*, 460–473.
- (21) Conrad, M. P.; Strauss, H. L. Nearly free rotation of water and ammonia in alkanes and other weakly interacting solvents. *J. Phys. Chem. A* 1987, *91*, 1668–1673.
- (22) Backx, P.; Goldman, S. H₂O/D₂O solubility isotope effects. An estimate of the extent of nonclassical rotational behavior of water, when dissolved in benzene or carbon tetrachloride. *J. Phys. Chem. A* **1981**, *85*, 2975–2979.
- (23) Śmiechowski, M. Unusual Influence of Fluorinated Anions on the Stretching Vibrations of Liquid Water. *J. Phys. Chem. B* **2018**, *122*, 3141–3152.
- (24) Irle, S.; Bowman, J. M. Direct *ab initio* variational calculation of vibrational energies of the H₂O···Cl⁻ complex and resolution of experimental differences. *J. Chem. Phys.* **2000**, *113*, 8401–8403.
- (25) Xantheas, S. S. Quantitative Description of Hydrogen Bonding in Chloride-Water Clusters. *J. Phys. Chem. A* **1996**, *100*, 9703–9713.
- (26) Thompson, W. H.; Hynes, J. T. Frequency Shifts in the Hydrogen-Bonded OH Stretch in Halide-Water Clusters. The Importance of Charge Transfer. J. Am. Chem. Soc. 2000, 122, 6278–6286.
- (27) Johnson, M. S.; Kuwata, K. T.; Wong, C.-K.; Okumura, M. Vibrational spectrum of $I^-(H_2O)$. Chem. Phys. Lett. **1996**, 260, 551–557.
- (28) Ayotte, P.; Kelley, J. A.; Nielsen, S. B.; Johnson, M. A. Vibrational spectroscopy of the F⁻·H₂O complex via argon predissociation: photoinduced, intracluster proton transfer? *Chem. Phys. Lett.* **2000**, *316*, 455–459.
- (29) Woronowicz, E. A.; Robertson, W. H.; Weddle, G. H.; Johnson, M. A.; Myshakin, E. M.; Jordan, K. D. Infrared Spectroscopic Characterization of the Symmetrical Hydration Motif in the SO₂⁻· H₂O Complex. *J. Phys. Chem. A* **2002**, *106*, 7086–7089.
- (30) Zhao, X. G.; Gonzalez-Lafont, A.; Truhlar, D. G.; Steckler, R. Molecular modeling of solvation. Cl⁻(D₂O). *J. Chem. Phys.* **1991**, *94*, 5544–5558.
- (31) Yates, B. F.; Schaefer, H. F.; Lee, T. J.; Rice, J. E. Infrared spectrum of F⁻·H₂O. *J. Am. Chem. Soc.* **1988**, *110*, 6327−6332.
- (32) Bentley, J.; Collins, J. Y.; Chipman, D. M. Dissociation of Ozonide in Water. J. Phys. Chem. A 2000, 104, 4629–4635.
- (33) Robertson, W. H.; Price, E. A.; Weber, J. M.; Shin, J.-W.; Weddle, G. H.; Johnson, M. A. Infrared Signatures of a Water Molecule Attached to Triatomic Domains of Molecular Anions: Evolution of the H-bonding Configuration with Domain Length. *J. Phys. Chem. A* **2003**, *107*, 6527–6532.
- (34) Surber, E.; Ananthavel, S. P.; Sanov, A. Nonexistent electron affinity of OCS and the stabilization of carbonyl sulfide anions by gas phase hydration. *J. Chem. Phys.* **2002**, *116*, 1920–1929.
- (35) Myshakin, E. M.; Jordan, K. D.; Sibert, E. L.; Johnson, M. A. Large anharmonic effects in the infrared spectra of the symmetrical $CH_3NO_2^-\cdot(H_2O)$ and $CH_3CO_2^-\cdot(H_2O)$ complexes. *J. Chem. Phys.* **2003**, *119*, 10138–10145.
- (36) Schneider, H.; Vogelhuber, K. M.; Weber, J. M. Infrared spectroscopy of anionic hydrated fluorobenzenes. *J. Chem. Phys.* **2007**, *127*, No. 114311.
- (37) Kelly, J. T.; Ellington, T. L.; Sexton, T. M.; Fortenberry, R. C.; Tschumper, G. S.; Asmis, K. R. Communication: Gas phase vibrational spectroscopy of the azide-water complex. *J. Chem. Phys.* **2018**, *149*, No. 191101.
- (38) Abdo, Y. A.; Tschumper, G. S. Competition between Solvent—Solvent and Solvent—Solute Interactions in the Microhydration of the Hexafluorophosphate Anion, $PF_6^-(H_2O)_{n=1,2}$. *J. Phys. Chem. A* **2020**, 124, 8744—8752.
- (39) Wang, Y.; Li, H.; Han, S. A Theoretical Investigation of the Interactions between Water Molecules and Ionic Liquids. *J. Phys. Chem. B* **2006**. *110*. 24646–24651.
- (40) Del Bene, J. E.; Alkorta, I.; Elguero, J. Microsolvation of the Be-F bond in complexes of BeF₂, BeF₃, and BeF₄²⁻ with nH₂O, for n = 1–6. *Mol. Phys.* **2021**, *119*, No. e1933637.

- (41) Wong, R. L.; Williams, E. R. Dissociation of $SO_4^{2-}(H_2O)_n$ Clusters, n = 3-17. J. Phys. Chem. A **2003**, 107, 10976–10983.
- (42) Lee, C.; Yang, W.; Parr, R. G. Development of the Colle-Salvetti correlation-energy formula into a functional of the electron density. *Phys. Rev. B* **1988**, *37*, 785–789.
- (43) Grimme, S.; Antony, J.; Ehrlich, S.; Krieg, H. A consistent and accurate *ab initio* parametrization of density functional dispersion correction (DFT-D) for the 94 elements H-Pu. *J. Chem. Phys.* **2010**, 132, No. 154104.
- (44) Zhao, Y.; Truhlar, D. G. The M06 suite of density functionals for main group thermochemistry, thermochemical kinetics, non-covalent interactions, excited states, and transition elements: two new functionals and systematic testing of four M06-class functionals and 12 other functionals. *Theor. Chem. Acc.* 2008, 120, 215–241.
- (45) Møller, C.; Plesset, M. S. Note on an Approximation Treatment for Many-Electron Systems. *Phys. Rev.* **1934**, *46*, 618–622.
- (46) Frisch, M. J.; Trucks, G. W.; Schlegel, H. B.; Scuseria, G. E.; Robb, M. A.; Cheeseman, J. R.; Scalmani, G.; Barone, V.; Petersson, G. A.; Nakatsuji, H.et al. *Gaussian 16*, revision C.01; Gaussian Inc: Wallingford CT, 2016.
- (47) Matthews, D. A.; Cheng, L.; Harding, M. E.; Lipparini, F.; Stopkowicz, S.; Jagau, T.-C.; Szalay, P. G.; Gauss, J.; Stanton, J. F. Coupled-cluster techniques for computational chemistry: The CFOUR program package. *J. Chem. Phys.* **2020**, *152*, No. 214108.
- (48) Bates, D. M.; Smith, J. R.; Janowski, T.; Tschumper, G. S. Development of a 3-body:many-body integrated fragmentation method for weakly bound clusters and application to water clusters $(H_2O)_{n=3-10,16,17}$. *J. Chem. Phys.* **2011**, *135*, No. 044123.
- (49) Bates, D. M.; Smith, J. R.; Tschumper, G. S. Efficient and Accurate Methods for the Geometry Optimization of Water Clusters: Application of Analytic Gradients for the 2-body:Many-Body QM:QM Fragmentation Method to $(H_2O)_n$, n=3-10. J. Chem. Theory Comput. 2011, 7, 2753–2760.
- (50) Howard, J. C.; Tschumper, G. S. N-body:Many-body QM:QM vibrational frequencies: Application to small hydrogen-bonded clusters. J. Chem. Phys. 2013, 139, No. 184113.
- (51) Howard, J. C.; Tschumper, G. S. Benchmark Structures and Harmonic Vibrational Frequencies Near the CCSD(T) Complete Basis Set Limit for Small Water Clusters: $(H_2O)_{n=2,3,4,5,6}$. *J. Chem. Theory Comput.* **2015**, *11*, 2126–2136.
- (52) Hopkins, B. W.; Tschumper, G. S. A multicentered approach to integrated QM/QM calculations. Applications to multiply hydrogen bonded systems. *J. Comput. Chem.* **2003**, *24*, 1563–1568.
- (53) Hopkins, B. W.; Tschumper, G. S. Multicentred QM/QM methods for overlapping model systems. *Mol. Phys.* **2005**, *103*, 309–315.
- (54) Hopkins, B. W.; Tschumper, G. S. Integrated quantum mechanical approaches for extended π systems: Multicentered QM/QM studies of the cyanogen and diacetylene trimers. *Chem. Phys. Lett.* **2005**, 407, 362–367.
- (55) Tschumper, G. S. Multicentered integrated QM:QM methods for weakly bound clusters: An efficient and accurate 2-body:many-body treatment of hydrogen bonding and van der Waals interactions. *Chem. Phys. Lett.* **2006**, 427, 185–191.
- (56) ElSohly, A. M.; Shaw, C. L.; Guice, M. E.; Smith, B. D.; Tschumper, G. S. Analytic gradients for the multicentred integrated QM:QM method for weakly bound clusters: efficient and accurate 2-body:many-body geometry optimizations. *Mol. Phys.* **2007**, *105*, 2777–2782.
- (57) Maseras, F.; Morokuma, K. IMOMM: A new integrated *ab initio* plus molecular mechanics geometry optimization scheme of equilibrium structures and transition-states. *J. Comput. Chem.* **1995**, *16*, 1170–1179.
- (58) Chung, L. W.; Hirao, H.; Li, X.; Morokuma, K. The ONIOM method: Its foundation and applications to metalloenzymes and photobiology. WIREs Comput. Mol. Sci. 2012, 2, 327–350.
- (59) Chung, L. W.; Sameera, W. M. C.; Ramozzi, R.; Page, A. J.; Hatanaka, M.; Petrova, G. P.; Harris, T. V.; Li, X.; Ke, Z.; Liu, F.; et al.

- The ONIOM Method and Its Applications. Chem. Rev. 2015, 115, 5678-5796.
- (60) Hankins, D.; Moskowitz, J. W.; Stillinger, F. H. Water Molecule Interactions. *J. Chem. Phys.* **1970**, *53*, 4544–4554.
- (61) Mayhall, N. J.; Raghavachari, K. Molecules-in-Molecules: An Extrapolated Fragment-Based Approach for Accurate Calculations on Large Molecules and Materials. *J. Chem. Theory Comput.* **2011**, 7, 1336–1343.
- (62) Saha, A.; Raghavachari, K. Dimers of Dimers (DOD): A New Fragment-Based Method Applied to Large Water Clusters. *J. Chem. Theory Comput.* **2014**, *10*, 58–67.
- (63) Saha, A.; Raghavachari, K. Analysis of Different Fragmentation Strategies on a Variety of Large Peptides: Implementation of a Low Level of Theory in Fragment-Based Methods Can Be a Crucial Factor. *J. Chem. Theory Comput.* **2015**, *11*, 2012–2023.
- (64) Jose, K. V. J.; Raghavachari, K. Evaluation of Energy Gradients and Infrared Vibrational Spectra through Molecules-in-Molecules Fragment-Based Approach. *J. Chem. Theory Comput.* **2015**, *11*, 950–961.
- (65) Jovan Jose, K. V.; Raghavachari, K. Molecules-in-molecules fragment-based method for the evaluation of Raman spectra of large molecules. *Mol. Phys.* **2015**, *113*, 3057–3066.
- (66) Jose, K. V. J.; Beckett, D.; Raghavachari, K. Vibrational Circular Dichroism Spectra for Large Molecules through Molecules-in-Molecules Fragment-Based Approach. *J. Chem. Theory Comput.* **2015**, *11*, 4238–4247.
- (67) Jovan Jose, K. V.; Raghavachari, K. Raman Optical Activity Spectra for Large Molecules through Molecules-in-Molecules Fragment-Based Approach. *J. Chem. Theory Comput.* **2016**, *12*, 585–594.
- (68) Jose, K. V. J.; Raghavachari, K. Fragment-Based Approach for the Evaluation of NMR Chemical Shifts for Large Biomolecules Incorporating the Effects of the Solvent Environment. *J. Chem. Theory Comput.* **2017**, *13*, 1147–1158.
- (69) Xantheas, S. S. Ab Initio Studies of Cyclic Water Clusters $(H_2O)_n$, n=1-6. II. Analysis of Many-Body Interactions. *J. Chem. Phys.* **1994**, 100, 7523–7534.
- (70) Elrod, M. J.; Saykally, R. J. Many-Body Effects in Intermolecular Forces. *Chem. Rev.* **1994**, *94*, 1975–1997.
- (71) Quack, M.; Suhm, M. A. Conceptual Perspectives in Quantum Chemistry; Calais, J.-L.; Kryachko, E. S., Eds.; Kluwer Pub. Co.: Dordrecht, 1997; Vol. III, pp 415–464.
- (72) Karpfen, A. Cooperative Effects in Hydrogen Bonding. Adv. Chem. Phys. 2002, 123, 469–510.
- (73) Gordon, M. S.; Fedorov, D. G.; Pruitt, S. R.; Slipchenko, L. V. Fragmentation Methods: A Route to Accurate Calculations on Large Systems. *Chem. Rev.* **2012**, *112*, 632–672.
- (74) Collins, M. A.; Bettens, R. P. A. Energy-Based Molecular Fragmentation Methods. *Chem. Rev.* **2015**, *115*, 5607–5642.
- (75) Raghavachari, K.; Saha, A. Accurate Composite and Fragment-Based Quantum Chemical Models for Large Molecules. *Chem. Rev.* **2015**, *115*, 5643–5677.
- (76) Richard, R. M.; Herbert, J. M. A generalized many-body expansion and a unified view of fragment-based methods in electronic structure theory. *J. Chem. Phys.* **2012**, *137*, No. 064113.
- (77) Richard, R. M.; Herbert, J. M. Many-Body Expansion with Overlapping Fragments: Analysis of Two Approaches. *J. Chem. Theory Comput.* **2013**, *9*, 1408–1416.
- (78) Richard, R. M.; Lao, K. U.; Herbert, J. M. Aiming for benchmark accuracy with the many-body expansion. *Acc. Chem. Res.* **2014**, *47*, 2828–2836.
- (79) Mayhall, N. J.; Raghavachari, K. Many-Overlapping-Body (MOB) Expansion: A Generalized Many Body Expansion for Nondisjoint Monomers in Molecular Fragmentation Calculations of Covalent Molecules. J. Chem. Theory Comput. 2012, 8, 2669–2675.
- (80) Day, P. N.; Jensen, J. H.; Gordon, M. S.; Webb, S. P.; Stevens, W. J.; Krauss, M.; Garmer, D.; Basch, H.; Cohen, D. An Effective Fragment Method for Modeling Solvent Effects in Quantum Mechanical Calculations. *J. Chem. Phys.* **1996**, *105*, 1968–1986.

- (81) Gordon, M. S.; Slipchenko, L.; Li, H.; Jensen, J. H. Chapter 10 The Effective Fragment Potential: A General Method for Predicting Intermolecular Interactions. *Ann. Rep. Comput. Chem.* **2007**, *3*, 177–193.
- (82) Pruitt, S. R.; Bertoni, C.; Brorsen, K. R.; Gordon, M. S. Efficient and accurate fragmentation methods. *Acc. Chem. Res.* **2014**, *47*, 2786–2794.
- (83) Kitaura, K.; Sawai, T.; Asada, T.; Nakano, T.; Uebayasi, M. Pair interaction molecular orbital method: an approximate computational method for molecular interactions. *Chem. Phys. Lett.* **1999**, 312, 319–324.
- (84) Kitaura, K.; Ikeo, E.; Asada, T.; Nakano, T.; Uebayasi, M. Fragment Molecular Orbital Method: An Approximate Computational Method for Large Molecules. *Chem. Phys. Lett.* **1999**, *313*, 701–706.
- (85) Fedorov, D. G.; Asada, N.; Nakanishi, I.; Kitaura, K. The Use of Many-Body Expansions and Geometry Optimizations in Fragment-Based Methods. *Acc. Chem. Res.* **2014**, *47*, 2846–2856.
- (86) Gadre, S. R.; Shirsat, R. N.; Limaye, A. C. Molecular Tailoring Approach for Simulation of Electrostatic Properties. *J. Phys. Chem. A* **1994**, 98, 9165–9169.
- (87) Sahu, N.; Gadre, S. R. Molecular Tailoring Approach: A Route for *ab Initio* Treatment of Large Clusters. *Acc. Chem. Res.* **2014**, 47, 2739–2747.
- (88) Hirata, S.; Valiev, M.; Dupuis, M.; Xantheas, S. S.; Sugiki, S.; Sekino, H. Fast electron correlation methods for molecular clusters in the ground and excited states. *Mol. Phys.* **2005**, *103*, 2255–2265.
- (89) Kamiya, M.; Hirata, S.; Valiev, M. Fast electron correlation methods for molecular clusters without basis set superposition errors. *J. Chem. Phys.* **2008**, *128*, No. 074103.
- (90) Hirata, S.; Gilliard, K.; He, X.; Li, J.; Sode, O. Ab Initio Molecular Crystal Structures, Spectra, and Phase Diagrams. *Acc. Chem. Res.* **2014**, *47*, 2721–2730.
- (91) Dahlke, E. E.; Truhlar, D. G. Electrostatically Embedded Many-Body Expansion for Large Systems, with Applications to Water Clusters. J. Chem. Theory Comput. 2007, 3, 46–53.
- (92) Dahlke, E. E.; Truhlar, D. G. Electrostatically Embedded Many-Body Correlation Energy, with Applications to the Calculation of Accurate Second-Order Møller-Plesset Perturbation Theory Energies for Large Water Clusters. *J. Chem. Theory Comput.* **2007**, *3*, 1342–1348.
- (93) Wang, B.; Yang, K. R.; Xu, X.; Isegawa, M.; Leverentz, H. R.; Truhlar, D. G. Quantum Mechanical Fragment Methods Based on Partitioning Atoms or Partitioning Coordinates. *Acc. Chem. Res.* **2014**, 47, 2731–2738.
- (94) Li, W.; Li, S.; Jiang, Y. Generalized Energy-Based Fragmentation Approach for Computing the Ground-State Energies and Properties of Large Molecules. *J. Phys. Chem. A* **2007**, *111*, 2193–2199.
- (95) Hua, W.; Fang, T.; Li, W.; Yu, J.-G.; Li, S. Geometry Optimizations and Vibrational Spectra of Large Molecules from a Generalized Energy-Based Fragmentation Approach. *J. Phys. Chem. A* **2008**, *112*, 10864–10872.
- (96) Li, S.; Li, W.; Ma, J. Generalized Energy-Based Fragmentation Approach and Its Applications to Macromolecules and Molecular Aggregates. *Acc. Chem. Res.* **2014**, *47*, 2712–2720.
- (97) Beran, G. J. O. Approximating quantum many-body intermolecular interactions in molecular clusters using classical polarizable force fields. *J. Chem. Phys.* **2009**, *130*, No. 164115.
- (98) Beran, G. J. O.; Nanda, K. Predicting Organic Crystal Lattice Energies with Chemical Accuracy. *J. Phys. Chem. Lett.* **2010**, *1*, 3480–3487
- (99) Nanda, K. D.; Beran, G. J. O. Prediction of organic molecular crystal geometries from MP2-level fragment quantum mechanical/molecular mechanical calculations. *J. Chem. Phys.* **2012**, *137*, No. 174106.
- (100) Guo, W.; Wu, A.; Xu, X. XO: An extended ONIOM method for accurate and efficient geometry optimization of large molecules. *Chem. Phys. Lett.* **2010**, 498, 203–208.

- (101) Guo, W.; Wu, A.; Zhang, I. Y.; Xu, X. XO: An extended ONIOM method for accurate and efficient modeling of large systems. *J. Comput. Chem.* **2012**, *33*, 2142–2160.
- (102) Xie, W.; Gao, J. Design of a Next Generation Force Field: The X-POL Potential. *J. Chem. Theory Comput.* **2007**, *3*, 1890–1900.
- (103) Wang, Y.; Sosa, C. P.; Cembran, A.; Truhlar, D. G.; Gao, J. Multilevel X-Pol: A Fragment-Based Method with Mixed Quantum Mechanical Representations of Different Fragments. *J. Phys. Chem. B* **2012**, *116*, 6781–6788.
- (104) Góra, U.; Podeszwa, R.; Cencek, W.; Szalewicz, K. Interaction energies of large clusters from many-body expansion. *J. Chem. Phys.* **2011**, *135*, No. 224102.
- (105) Dunning, T. H. Gaussian basis sets for use in correlated molecular calculations. I. The atoms boron through neon and hydrogen. *J. Chem. Phys.* **1989**, *90*, 1007–1023.
- (106) Kendall, R. A.; Dunning, T. H.; Harrison, R. J. Electron affinities of the first-row atoms revisited. Systematic basis sets and wave functions. *J. Chem. Phys.* **1992**, *96*, 6796–6806.
- (107) Del Bene, J. E. Proton affinities of ammonia, water, and hydrogen fluoride and their anions: a quest for the basis-set limit using the Dunning augmented correlation-consistent basis sets. *J. Phys. Chem. A* **1993**, *97*, 107–110.
- (108) Del Bene, J. E.; Shavitt, I. Basis-set effects on computed acid-base interaction energies using the Dunning correlation-consistent polarized split-valence basis sets. *J. Mol. Structure THEOCHEM* **1994**, 307, 27–34.
- (109) Tschumper, G. S.; Leininger, M. L.; Hoffman, B. C.; Valeev, E. F.; Schaefer, H. F.; Quack, M. Anchoring the water dimer potential energy surface with explicitly correlated computations and focal point analyses. *J. Chem. Phys.* **2002**, *116*, 690–701.
- (110) Anderson, J. A.; Crager, K.; Fedoroff, L.; Tschumper, G. S. Anchoring the potential energy surface of the cyclic water trimer. *J. Chem. Phys.* **2004**, *121*, 11023–11029.
- (111) Tschumper, G. S. Reviews in Computational Chemistry; John Wiley & Sons, Ltd, 2008; Chapter 2, pp 39–90.
- (112) Sullivan, M. B.; Iron, M. A.; Redfern, P. C.; Martin, J. M. L.; Curtiss, L. A.; Radom, L. Heats of Formation of Alkali Metal and Alkaline Earth Metal Oxides and Hydroxides: Surprisingly Demanding Targets for High-Level ab Initio Procedures. *J. Phys. Chem. A* **2003**, *107*, 5617–5630.
- (113) Bates, D. M.; Anderson, J. A.; Oloyede, P.; Tschumper, G. S. Probing the effects of heterogeneity on delocalized $\pi \cdots \pi$ interaction energies. *Phys. Chem. Chem. Phys.* **2008**, *10*, 2775–2779.
- (114) ElSohly, A. M.; Tschumper, G. S. Comparison of polarization consistent and correlation consistent basis sets for noncovalent interactions. *Int. J. Quantum Chem.* **2009**, *109*, 91–96.
- (115) Bates, D. M.; Tschumper, G. S. CCSD(T) Complete Basis Set Limit Relative Energies for Low-Lying Water Hexamer Structures. *J. Phys. Chem. A* **2009**, *113*, 3555–3559.
- (116) Marshall, M. S.; Burns, L. A.; Sherrill, C. D. Basis set convergence of the coupled-cluster correction, $\delta_{\mathrm{MP2}}^{\mathrm{CCSD}(\mathrm{T})} \delta_{\mathrm{MP2}}^{\mathrm{CCSD}(\mathrm{T})}$: Best practices for benchmarking non-covalent interactions and the attendant revision of the S22, NBC10, HBC6, and HSG databases. *J. Chem. Phys.* **2011**, 135, 194102.
- (117) Řezáč, J.; Riley, K. E.; Hobza, P. Extensions of the S66 Data Set: More Accurate Interaction Energies and Angular-Displaced Nonequilibrium Geometries. *J. Chem. Theory Comput.* **2011**, *7*, 3466—3470.
- (118) Řezáč, J.; Riley, K. E.; Hobza, P. Benchmark Calculations of Noncovalent Interactions of Halogenated Molecules. *J. Chem. Theory Comput.* **2012**, *8*, 4285–4292.
- (119) Brauer, B.; Kesharwani, M. K.; Kozuch, S.; Martin, J. M. L. The 866×8 benchmark for noncovalent interactions revisited: explicitly correlated ab initio methods and density functional theory. *Phys. Chem. Chem. Phys.* **2016**, *18*, 20905–20925.
- (120) Manna, D.; Kesharwani, M. K.; Sylvetsky, N.; Martin, J. M. L. Conventional and Explicitly Correlated ab Initio Benchmark Study on Water Clusters: Revision of the BEGDB and WATER27 Data Sets. J. Chem. Theory Comput. 2017, 13, 3136–3152.

- (121) Kesharwani, M. K.; Manna, D.; Sylvetsky, N.; Martin, J. M. L. The X40 \times 10 Halogen Bonding Benchmark Revisited: Surprising Importance of (n-1)d Subvalence Correlation. *J. Phys. Chem. A* **2018**, 122, 2184–2197.
- (122) Papajak, E.; Truhlar, D. G. Convergent Partially Augmented Basis Sets for Post-Hartree-Fock Calculations of Molecular Properties and Reaction Barrier Heights. *J. Chem. Theory Comput.* **2011**, *7*, 10–18.
- (123) Papajak, E.; Zheng, J.; Xu, X.; Leverentz, H. R.; Truhlar, D. G. Perspectives on Basis Sets Beautiful: Seasonal Plantings of Diffuse Basis Functions. *J. Chem. Theory Comput.* **2011**, *7*, 3027–3034.
- (124) Liu, B.; McLean, A. D. Accurate calculation of the attractive interaction of two ground state helium atoms. *J. Chem. Phys.* **1973**, *59*, 4557–4558.
- (125) Kestner, N. R. He-He Interaction in the SCF-MO Approximation. J. Chem. Phys. 1968, 48, 252-257.
- (126) Jansen, H.; Ros, P. Non-empirical molecular orbital calculations on the protonation of carbon monoxide. *Chem. Phys. Lett.* **1969**, 3, 140–143.
- (127) Boys, S.; Bernardi, F. The calculation of small molecular interactions by the differences of separate total energies. Some procedures with reduced errors. *Mol. Phys.* **1970**, *19*, 553–566.
- (128) Dornshuld, E. V.; Holy, C. M.; Tschumper, G. S. Homogeneous and Heterogeneous Noncovalent Dimers of Formaldehyde and Thioformaldehyde: Structures, Energetics, and Vibrational Frequencies. *J. Phys. Chem. A* **2014**, *118*, 3376–3385. PMID: 24766482.
- (129) Weber, J. M.; Kelley, J. A.; Robertson, W. H.; Johnson, M. A. Hydration of a structured excess charge distribution: Infrared spectroscopy of the $O_2^-(H_2O)_n$, $(1 \le n \le 5)$ clusters. *J. Chem. Phys.* **2001**, *114*, 2698–2706.
- (130) Myshakin, E. M.; Jordan, K. D.; Robertson, W. H.; Weddle, G. H.; Johnson, M. A. Dominant structural motifs of $NO^-(H_2O)_n$ complexes: Infrared spectroscopic and ab initio studies. *J. Chem. Phys.* **2003**, *118*, 4945–4953.
- (131) Robertson, W. H.; Diken, E. G.; Price, E. A.; Shin, J.-W.; Johnson, M. A. Spectroscopic Determination of the OH⁻ Solvation Shell in the OH⁻ (H₂O)_n Clusters. *Science* **2003**, 299, 1367–1372.
- (132) Wang, X.-B.; Kowalski, K.; Wang, L.-S.; Xantheas, S. S. Stepwise hydration of the cyanide anion: A temperature-controlled photoelectron spectroscopy and ab initio computational study of $CN^-(H_2O)_n$, n=2-5. *J. Chem. Phys.* **2010**, *132*, No. 124306.
- (133) Gorlova, O.; DePalma, J. W.; Wolke, C. T.; Brathwaite, A.; Odbadrakh, T. T.; Jordan, K. D.; McCoy, A. B.; Johnson, M. A. Characterization of the primary hydration shell of the hydroxide ion with H_2 tagging vibrational spectroscopy of the $OH^-(H_2O)_{n=2,3}$ and $OD^-(D_2O)_{n=2,3}$ clusters. *J. Chem. Phys.* **2016**, *145*, No. 134304.
- (134) Feyereisen, M. W.; Feller, D.; Dixon, D. A. Hydrogen Bond Energy of the Water Dimer. *J. Phys. Chem. A* **1996**, *100*, 2993–2997. (135) Howard, J. C.; Gray, J. L.; Hardwick, A. J.; Nguyen, L. T.; Tschumper, G. S. Getting down to the Fundamentals of Hydrogen Bonding: Anharmonic Vibrational Frequencies of (HF)₂ and (H₂O)₂ from Ab Initio Electronic Structure Computations. *J. Chem. Theory Comput.* **2014**, *10*, 5426–5435.